

1 **Emission characteristics of reactive organic gases from**
2 **industrial volatile chemical products (VCPs) in the Pearl**
3 **River Delta (PRD), China**

4 **Sihang Wang¹, Bin Yuan^{1,*}, Xianjun He¹, Ru Cui^{1,a}, Xin Song¹, Yubin Chen¹,**
5 **Caihong Wu¹, Chaomin Wang¹, Yibo Huangfu¹, Xiao-Bing Li¹, Boguang Wang¹,**
6 **Min Shao¹**

7 ¹ College of Environment and Climate, Institute for Environmental and Climate
8 Research, Guangdong-Hongkong-Macau Joint Laboratory of Collaborative Innovation
9 for Environmental Quality, Jinan University, Guangzhou 511443, China

10 ^a now at: Nanjing Intelligent Environmental Science and Technology Co.Ltd, Nanjing
11 211800, China

12
13 *Email: byuan@jnu.edu.cn
14
15

删除了: ²

删除了: ²

删除了: ²

删除了: ²

删除了: ²

删除了: ²

删除了: ²

删除了: ²

删除了: ²

删除了: ²

删除了: ²

删除了: ²

删除了: Institute

删除了: for Environmental and Climate Research, Jinan University

删除了: ² Guangdong-Hongkong-Macau Joint Laboratory of Collaborative Innovation for Environmental Quality, Guangzhou 511443, China

35 **Abstract:**

36 Volatile chemical products (VCPs) have become an important source of reactive
37 organic gases (ROGs) in urban areas worldwide. Industrial activities can also utilize a
38 large amount of VCPs and emit many organic gases into the atmosphere. Due to
39 multiple sampling and measurement challenges, only a subset of ROG species is usually
40 measured for many industrial VCP sources. This study aimed to investigate the
41 emissions of ROGs from five industrial VCP sources in the Pearl River Delta (PRD)
42 region of China, including shoemaking, plastic surface coating, furniture coating,
43 printing, and ship coating industries. More comprehensive speciation of ROG
44 emissions from these industrial VCP sources was developed by the combination of the
45 proton transfer reaction time-of-flight mass spectrometer (PTR-ToF-MS) along with
46 gas chromatography-mass spectrometer/flame ionization detector (GC-MS/FID). Our
47 study identified oxygenated ROG species (OVOCs) as representative ROGs emitted
48 from these sources, which are highly related to specific chemicals used during the
49 industrial activities. Moreover, mass spectra similarity analysis revealed significant
50 dissimilarities among the ROG emission from industrial activities, indicating
51 substantial variations between different industrial VCP sources. Except for the ship
52 coating industry utilizing solvent-borne coatings, the proportions of OVOCs range from
53 67% to 96% in total ROG emissions and 72% to 97% in total OH reactivity (OHR) for
54 different industrial sources, while the corresponding contributions of OVOCs in the
55 ship coating industry are only 16%±3.5% and 15%±3.6%. The industrial VCP sources
56 associated with solvent-borne coatings exhibited a higher ozone formation potential
57 (OFP), reaching as high as 5.5 and 2.7 g O₃·g⁻¹ ROGs for ship coating and furniture
58 coating industries, primarily due to contributions from aromatics. We find that a few
59 species can contribute the majority of the ROG emissions, and also their OHR and OFP
60 from various industrial VCP sources. Our results suggest that ROG treatment devices
61 may have limited effectiveness for all ROGs, with treatment efficiencies ranging from
62 -12% to 68%. Furthermore, we found that ambient measurements in industrial areas
63 have been significantly impacted by industrial VCP sources, and ROG pairs (e.g.,

删除了: sources

删除了: The fractions of the ten most abundant species in total ROG emissions, OHR, and OFP indicated a highly centralized of ROG emissions from various industrial VCP sources....

69 methyl ethyl ketone (MEK) /C₈ aromatics ratio) ~~can be utilized as reliable evidence by~~
70 ~~using high time-resolution ROG measurements from PTR-ToF-MS.~~ Our study
71 demonstrated the importance of measuring a large number of ROGs using PTR-ToF-
72 MS for characterizing ROG emissions from industrial VCP sources.
73

删除了: could serve as effective

删除了: indicators for distinguishing industrial VCP sources, particularly for measurements in industrial areas

77 1. Introduction

78 With the successful control of vehicular emissions, emission from volatile
79 chemical products (VCPs) have become an increasingly significant source in cities all
80 around the world (Sun et al., 2018;McDonald et al., 2018;Li et al., 2019;Khare and
81 Gentner, 2018;Seltzer et al., 2022;Sasidharan et al., 2023). Reactive organic gases
82 (ROGs), organic gases other than methane, from VCPs emission can contribute
83 substantially to both anthropogenic secondary organic aerosol (SOA) and ozone (O₃)
84 in urban environments (Seltzer et al., 2022;Khare et al., 2022;Sasidharan et al.,
85 2023;Coggon et al., 2021;Gkatzelis et al., 2021b;Qin et al., 2021). With the
86 development of economy and industrialization, the emissions of industrial VCPs
87 contribute to approximately 25%-45% of ROG emissions in China (Ou et al., 2015;Wei
88 et al., 2011;Huang et al., 2011;Sha et al., 2021;Zhou et al., 2020b). To effectively
89 control atmospheric pollution in urban areas and surrounding regions, it becomes
90 imperative to gain a comprehensive understanding of the emission characteristics of
91 ROGs from industrial VCP sources.

92 Extensive research has been conducted to investigate ROG emissions from
93 industrial VCP sources, mainly focusing on sampling within manufacturing workshops
94 and exhaust stacks (Zheng et al., 2013;Yuan et al., 2010;Wang et al., 2014). Previous
95 studies have demonstrated that the use of individual chemicals (i.e. coatings, inks, and
96 adhesives) significantly impact ROG emissions (Gkatzelis et al., 2021a;Zheng et al.,
97 2013;He et al., 2022a), and these chemicals used for printing, furniture, and shoemaking
98 industries has seen rapid growth and widespread adoption in recent years (Gkatzelis et
99 al., 2021a;McDonald et al., 2018;Seltzer et al., 2022;Coggon et al., 2021). Consequently,
100 the diverse emission sources and emission factors from industrial VCP sources have
101 contributed to large uncertainties (Mo et al., 2021;Zhong et al., 2018). To mitigate the
102 emissions of most primary pollutants, stricter emission standards have been
103 implemented along with advancements in ROG treatment technologies in China.
104 Specifically, water-borne VCPs has substituted solvent-borne VCPs in several
105 industries, such as printing, interior wall coating, and automotive manufacturing.

删除了: on

删除了: in China

108 However, the replacement in steel structures, automotive plastic parts manufacturing
109 and ship building industries remains below 3% (Mo et al., 2021;Li et al., 2019;Shi et
110 al., 2023;Wang et al., 2023). As a result, the emission characteristics of ROGs from
111 industrial VCP sources may undergo changes in response to the ongoing development
112 of VCPs and ROG treatment technologies. It is imperative to regularly updated the
113 understanding of ROG emission characteristics associated with industrial VCP sources.

114 The emissions of oxygenated ROG species (OVOCs) have been identified as
115 significant components in industrial VCP emissions (Chang et al., 2022;Mo et al.,
116 2021;Sha et al., 2021). For instance, it has been found that more than 80% of total ROG
117 emissions for shoemaking and printing industries are attributed to OVOC emissions
118 (Zheng et al., 2013). This notable contributions of OVOCs, such as acetone, methyl
119 ethyl ketone (MEK), ethyl acetate, and isopropanol, can be primarily attributed to the
120 use of individual industrial chemicals (Zheng et al., 2013;Wu et al., 2020b).
121 Traditionally, the collection of ROGs involved the use of canisters or Tedlar bags, and
122 their analysis was conducted using gas chromatography-mass spectrometer/flame
123 ionization detector (GC-MS/FID) techniques, with a primary focus on hydrocarbon
124 emissions (Yuan et al., 2010;Wang et al., 2014). Previous studies commonly employed
125 2,4-dinitrophenylhydrazine (DNPH) cartridges for collection and analyzed them using
126 high-performance liquid chromatography (HPLC) to detect carbonyl species such as
127 aldehydes and ketones. However, this approach is both time-consuming and susceptible
128 to contaminations (Mo et al., 2016;Han et al., 2019).

129 Due to the intricate chemical compositions of industrial VCPs, it is essential to
130 characterize ROG emissions with higher mass resolution. The proton-transfer-reaction
131 time-of-flight mass spectrometer (PTR-ToF-MS) has been extensively utilized for the
132 identification of VCP sources. More evidence shows that the contribution of VCP
133 sources to anthropogenic ROG emissions is gradually becoming more prominent. For
134 instance, ROG emissions from VCP contribute 50%-80% of anthropogenic ROG
135 emissions in US cities (Gkatzelis et al., 2021b;McDonald et al., 2018). The large
136 fractions (~50%) of ROGs have been attributed to a VCP-dominated source in

删除了: It has been confirmed that VCP sources is a significant contributor to ROG emissions.

139 Guangzhou, highlighting its importance in urban environments (Li et al., 2022).
140 Through high mass resolution analysis, tracer compounds for various VCP categories
141 have been identified (Gkatzelis et al., 2021a; Coggon et al., 2018; Stockwell et al., 2021).
142 In addition, OVOCs such as acetates, acrylates, alcohols (e.g. benzyl alcohol), glycols
143 (e.g. propylene glycol, ethylene glycol), and glycol ethers, have been found to make
144 significant contributions to VCPs emission (Seltzer et al., 2021; Li and Cocker, 2018; Li
145 et al., 2018; Khare et al., 2022). With the ability to measure whole mass spectra and
146 offer high mass resolution, the PTR-ToF-MS enables more comprehensive detection of
147 a wide range of ROGs (Cappellin et al., 2012; Yuan et al., 2017; Huangfu et al., 2021).
148 By employing parameterization methods to determine instrument sensitivity, more
149 ROGs can be quantified from the obtained mass spectra (Sekimoto et al., 2017; Wu et
150 al., 2020a). Furthermore, previous studies have demonstrated that higher alkanes,
151 including acyclic, cyclic and bicyclic alkanes can be measured using PTR-ToF-MS with
152 NO^+ chemical ionization (NO^+ PTR-ToF-MS) (Inomata et al., 2014; Koss et al.,
153 2016; Wang et al., 2020; Chen et al., 2022). Higher alkanes are significant species in
154 vehicle and combustion emissions (Gao et al., 2023; Liu et al., 2021; Zhao et al., 2018b),
155 and they were not included in previous measurements of industrial VCP sources. Thus,
156 by combining hydrocarbons measured by offline GC-MS/FID, PTR-ToF-MS shows
157 promise as a method for developing more comprehensive speciation relevant to
158 industrial VCP emissions (Gao et al., 2023).

159 In this study, we applied a PTR-ToF-MS employing H_3O^+ and NO^+ chemical
160 ionization along with a GC-MS/FID to comprehensively measure ROG emissions from
161 five industrial VCP sources, including shoemaking, plastic surface coating, furniture
162 coating, printing, and ship coating industries in the PRD region of China. We
163 investigated emission characteristics of ROGs across these industries, and utilized the
164 dataset to analyze the contributions of different ROG components to total ROG
165 emissions, OH reactivity (OHR), ozone formation potential (OFP), and volatility in
166 various industrial VCP sources. Furthermore, we conducted intercomparisons of the
167 mass spectra characterizations of ROG emissions, which revealed significant variations

删除了: Pearl River Delta (PRD)

删除了: from semi-open workshops and ROG treatment devices across these industries. We

171 in ROG emissions from industrial VCP sources.

172 2. Materials and methods

173 2.1 Tested industrial VCP sources and sampling methods

174 Based on comprehensive analysis of written data, consultation with relevant
175 experts, and thorough on-site investigations, we selected five representative factories
176 and industries from various industrial VCP sources. The selection criteria for these
177 industries were based on relevant emission inventory research conducted in the PRD
178 region of China (Zhong et al., 2018). Sampling methods focused on capturing ROG
179 emissions generated during the main manufacturing processes, such as coatings
180 spraying and adhesives usage in the factories. Both online measurements and offline
181 sampling were carried out in semi-open workshops, as well as ROG treatment devices
182 (i.e. before and after emission treatment, generally located at the front and rear sampling
183 ports of the ROG treatment devices) in the factories (Table. S1).

184 Typically, workshop waste gases are routed through collection devices (e.g. gas-
185 collecting hoods, airtight partitions), and then processed in ROG treatment devices (e.g.
186 ultraviolet-ray (UV) oxidation, activated carbon adsorption, combustion, and
187 biodegradation). These treated gases are then released into the atmosphere through
188 exhaust stacks. ROG treatment devices play a crucial role in reducing ROG emissions
189 by employing recovery and destruction technologies (Wang et al., 2023;Kamal et al.,
190 2016). Recovery processes involve enriching and separating VOCs by means of
191 temperature or pressure changes and selective absorbents, while destruction processes
192 converts VOCs into harmless substances such as CO₂ and H₂O through combustion
193 (Wang et al., 2023). In this study, we evaluate two types of ROG treatment devices:
194 activated carbon adsorption combined with UV photolysis devices (installed in
195 shoemaking, plastic surface coating, furniture coating, and printing industries) and
196 catalytic combustion devices (installed in printing and ship coating industries).

197 During the campaign, a mobile monitoring vehicle was equipped with online
198 measurement equipment and strategically parked near the sampling ports of both
199 workshops and ROG treatment devices emissions (Fig. S1). A CO₂ / H₂O gas analyzer

删除了:

删除了:

202 (LI-COR 840A, Inc., USA) was used to measure the concentrations of CO₂ and H₂O.
203 To ensure continuous sampling, air from various factories was drawn through a length
204 of Perfluoroalkoxy (PFA) Teflon tubing, ranging from 10 to 100 meters, at a controlled
205 flow rate of 6 L/min facilitated by an external pump. The use of long tubing was
206 assessed through laboratory tests, which showed that the tubing had a negligible and
207 minor influence on most ROG species. This confirmed the feasibility of measurement
208 using long PFA tubing, more detail can be found elsewhere (Li et al., 2023).

209 **2.2 ROG measurements**

210 In this study, ROG were measured using a proton transfer reaction quadrupole
211 interface time-of-flight mass spectrometer (PTR-QiToF-MS) (IONICON Analytik,
212 Innsbruck, Austria) (Sulzer et al., 2014) and a combination of canister sampling and
213 offline GC-MS/FID analysis system (canister-GC-MS/FID). More comprehensive
214 speciation of ROG was achieved by analyzing hydrocarbons by canister-GC-MS/FID,
215 quantifying all signals using H₃O⁺ PTR-ToF-MS, and supplementing by acyclic, cyclic,
216 and bicyclic alkanes from NO⁺ ionization of PTR-ToF-MS. The selection of
217 overlapping ROGs was similar to a previous study (Table. S2) (Gao et al., 2023).

218 To capture the real-time emission characteristics of ROGs from industrial VCP
219 sources, the mass spectra of PTR-ToF-MS was recorded every 10 s. Prior to each test,
220 background measurements of the instrument were carried out by passing sampling air
221 through a custom-built platinum catalytical converter that had been preheated to 365 °C
222 for 1 minute. Throughout the campaign, the PTR-ToF-MS instrument automatically
223 alternated between two reagent ions (H₃O⁺ and NO⁺) every 10 minutes. Detailed setting
224 parameters for H₃O⁺ and NO⁺ chemical modes in this instrument can be found in
225 previous studies (Wu et al., 2020a; Wang et al., 2020; He et al., 2022b). The Tofware
226 software package (version 3.0.3, Tofwerk AG, Switzerland) was employed to facilitate
227 accurate data analysis (Stark et al., 2015).

228 Calibration for ROGs measure by PTR-ToF-MS were carried out both in the
229 laboratory and during the campaign. The PTR-ToF-MS was regularly calibrated using
230 a 23-component gas standard (Linde Spectra) throughout the campaign. During the later

231 period of the campaign, two gas standards (Apel Riemer Environmental Inc.) were used
232 for the calibration of other ROGs, specifically for acyclic and cyclic alkanes using NO⁺
233 chemical ionization. (Wang et al., 2020;Chen et al., 2022;Wang et al., 2022). A total of
234 11 organic acids and nitrogen-containing compounds were calibrated using the liquid
235 calibration unit (LCU, IONICON Analytik, Innsbruck, Austria) (Table. S3-S5). In order
236 to account for the humidity dependence of some ROGs in the PTR-ToF-MS (Yuan et
237 al., 2017;Koss et al., 2018), humidity-dependence curves established in the laboratory
238 were utilized for correction (Wu et al., 2020a;He et al., 2022b;Wang et al., 2022).
239 Sensitivities of uncalibrated species were determined based on the kinetics of proton-
240 transfer reactions of H₃O⁺ with ROGs (Fig. S2) (Cappellin et al., 2012;Sekimoto et al.,
241 2017), with an associated uncertainty of approximately 50% for the concentrations of
242 uncalibrated species.

243 Simultaneously, offline sampling was conducted near the sampling ports of
244 workshops and ROG treatment devices. Whole air samples were collected using
245 canisters for determination of hydrocarbons in industrial VCP sources, and analyzed by
246 an offline GC-MS/FID system. The GC-MS/FID system was calibrated using
247 photochemical assessment monitoring stations (PAMS) and TO-15 standard mixtures,
248 which enabled the identification and quantification of a total of 94 hydrocarbons. More
249 information about this instrument and dataset for canister sampling and offline GC-
250 MS/FID system can be found elsewhere (Li et al., 2020).

251 **2.3 Calibrations of esters and isopropanol based on H₃O⁺ and NO⁺** 252 **ionization**

253 Since ester species (including acetates and acrylates) play a significant role in
254 industrial VCP sources, it is important to accurately quantify their concentrations
255 (Khare et al., 2022). Previous studies have demonstrated that ethyl acetate exhibits
256 notable fragmentation, resulting in interference at m/z 61 (e.g. C₂H₄O₂H⁺) and m/z 43
257 (e.g. C₂H₂OH⁺) (Haase et al., 2012;de Gouw and Warneke, 2007;Rogers et al.,
258 2006;Fortner et al., 2009). Therefore, we employed the PTR-ToF-MS to directly
259 measure high-purity ester chemicals and identify the characteristic product ions

删除了: 2

删除了: 4

删除了:

删除了:.

264 produced by esters under H_3O^+ and NO^+ chemical ionization. Several common esters
265 including methyl acetate, ethyl acetate, isopropyl acetate, and vinyl acetate, were
266 selected to investigate instrument fragmentation under different ionizations. As shown
267 in Table. S6, it is intriguing to observe that high-molecular-weight acetates tend to
268 exhibit more fragmentation, resulting in interference at m/z 61 (e.g. $\text{C}_2\text{H}_4\text{O}_2\text{H}^+$) and m/z
269 43 (e.g. $\text{C}_2\text{H}_2\text{OH}^+$). Methyl acetate (95%) and ethyl acetate (72%) displayed limited
270 fragmentation in the instrument, while isopropyl acetate accounted for only 13% of the
271 $\text{C}_3\text{H}_{10}\text{O}_2\text{H}^+$ ions. Additionally, esters with different chemical structures may undergo
272 distinct modes of fragmentation. For example, vinyl acetate primarily fragmented to
273 produce interfering fragments at m/z 43 (e.g. $\text{C}_2\text{H}_2\text{OH}^+$) with a fraction of 78%.
274 Furthermore, considering the PTR-ToF-MS mass spectra from various industrial VCP
275 sources, it is conceivable that other ester compounds might also contribute to these mass
276 channels, emphasizing the need for cautious consideration of m/z 61 (e.g. $\text{C}_2\text{H}_4\text{O}_2\text{H}^+$)
277 and m/z 43 (e.g. $\text{C}_2\text{H}_2\text{OH}^+$) signals measured by H_3O^+ PTR-ToF-MS in industrial VCP
278 sources. The use of NO^+ chemical ionization exhibits various reaction pathways with
279 ROGs (Wang et al., 2020; Chen et al., 2022), which can partially mitigate interference
280 from fragment ions (Table. S6). The identified results of acetates based on NO^+
281 ionization demonstrated considerable improvements for methyl acetate (83%) and ethyl
282 acetate (80%), whereas vinyl acetate exhibited more fragmentation, with the largest
283 contribution (47%) at m/z 43 (e.g. $\text{C}_2\text{H}_2\text{OH}^+$).

284 Additionally, it is challenging to calibrate isopropanol in the H_3O^+ PTR-ToF-MS
285 since alcohols split off water during ionization (Buhr et al., 2002). To overcome this
286 challenge, we implemented daily calibrations of isopropanol under ambient humidity
287 conditions throughout the campaign (Fig. S3). The NO^+ PTR-ToF-MS was also
288 employed to calibrate isopropanol by identifying the characteristic product ions
289 produced under NO^+ ionization (Table. S6). The dominating product ion of isopropanol
290 was observed at m/z 59 (e.g. $\text{C}_3\text{H}_7\text{O}^+$) (88%), which corresponds to acetone ($\text{C}_3\text{H}_6\text{OH}^+$)
291 ions in the H_3O^+ PTR-ToF-MS. Although the dominant product ion for acetone under
292 NO^+ ionization was observed at m/z 88 (e.g. $\text{C}_3\text{H}_6\text{O}(\text{NO})^+$) (77%), the interfere at m/z

删除了: 5

删除了: 5

删除了: This result could be explained by the instrument was more likely to have a fracture reaction due to the chemical structure of vinyl acetate, which contains a C=C bond....

删除了: 5

300 59 (e.g. $C_3H_6OH^+$) (23%) was not insignificant. Therefore, the concentration of
301 isopropanol measured by NO^+ PTR-ToF-MS in this campaign has eliminated the
302 influence of acetone. Finally, the comparison between PTR-ToF-MS with H_3O^+ and
303 NO^+ chemical ionization is shown in Fig. S4-S5. Previous studies have shown good
304 agreement between measurements obtained using PTR-ToF-MS with H_3O^+ and NO^+
305 chemical ionization in ambient measurements (Wang et al., 2020). However, a slightly
306 weaker correlation was observed in industrial VCP sources, potentially due to the large
307 changes for different species between the switch of the two reagent ions. Our results
308 demonstrated that the NO^+ PTR-ToF-MS can also provide a complementary approach
309 for characterizing ester species and isopropanol in ambient air as well as emission
310 sources.

311 2.4 Mass spectra similarity analysis

312 We conducted a comprehensive comparison of various ROG emission sources by
313 considering the entire range of species in mass spectra as dimensions in a vector, and
314 calculating the cosine angle (θ) similarity (Humes et al., 2022;Ulbrich et al.,
315 2009;Kostenidou et al., 2009). The angle θ between the two mass spectra (MS_a and MS_b)
316 is given by the following:

$$317 \quad \cos \theta = \frac{MS_a MS_b}{|MS_a||MS_b|} \quad (1)$$

318 The θ angles between two mass spectra is divided into 4 groups, including 0° -
319 15° , 15° - 30° , 30° - 50° , and $>50^\circ$, which correspond to excellent consistency, good
320 consistency, many similarities, and poor consistency, respectively. Due to the distinct
321 ionization methods of the instruments, our classification of angle similarity is not as
322 strict as that reported in previous studies (Kostenidou et al., 2009;Zhu et al., 2021). As
323 these previous studies utilize the similarity analysis on mass spectra of aerosol mass
324 spectrometer (AMS) obtained from electron ionization, leading to very similar mass
325 spectra for different sources.

326 3. Results and discussions

327 3.1 Time-resolved ROG emissions from industrial VCP sources

删除了: Finally, the good agreement between measurements obtained using PTR-ToF-MS with H_3O^+ and NO^+ chemical ionization throughout the campaign indicates that the NO^+ PTR-ToF-MS can serve as a reliable method for measuring isopropanol and ester species in industrial VCP sources (Fig. S4-S5). ...

334 Time series of several ROGs measured by the H_3O^+ PTR-ToF-MS from five
335 industrial VCP sources are shown in Fig. 1 and Fig. S6. More information for these
336 sources can be found in Sect. S1 in the Supplement. Online measurements were carried
337 out in semi-open workshops (workshops emission) and from ROG treatment devices
338 (i.e. before and after treatment emission). As the waste gas was directly discharged into
339 the ambient air from exhaust stacks, the after treatment emission was can be considered
340 as stack emission (Zheng et al., 2013). The average concentrations of eight
341 representative ROGs, including aromatics, ketones, alcohols, and esters, between
342 workshops emission and stack emission for all factories is presented in Fig. S7. The
343 evaluation of the ROGs treatment efficiency is based on the analysis of emission
344 characteristics before and after treatment in the ROG treatment devices, which is
345 discussed in greater detail in Section 3.3. Along with the typical ROGs, the PTR-ToF-
346 MS measured a wide range of ions in abundance in the mass spectra. Fig. 2 displays
347 mass spectra representing the average concentrations of stack emissions from five
348 industrial VCP sources for all detected ROGs. These ROGs measured by the PTR-ToF-
349 MS were categorized based on their chemical formula, namely hydrocarbon species
350 (C_xH_y), OVOCs ($\text{C}_x\text{H}_y\text{O}_1$, $\text{C}_x\text{H}_y\text{O}_2$, and $\text{C}_x\text{H}_y\text{O}_{\geq 3}$), species containing nitrogen and/or
351 sulfur atoms (N/S-containing), species containing siloxanes (Si-containing), and other
352 ions (others).

353 3.1.1 Emission characteristics from industrial VCP sources

354 A. Shoemaking industry

355 Real-time concentrations of toluene, acetone, ethyl acetate, and isopropanol from
356 the shoemaking industry are displayed in Fig. 1a. The variable manufacturing processes
357 conditions are demonstrated by inconsistent emission levels in the workshops. This
358 variation may be attributed to different emission intensities during different periods.
359 Notably, the significant emissions from the shoemaking industry are primarily
360 attributed to a few low-molecular-weight OVOCs (Fig. 2a), including acetone, MEK,
361 isopropanol, and formaldehyde, followed by a fraction of hydrocarbon species (e.g.
362 toluene). Our results align with previous findings (Zheng et al., 2013; Zhao et al., 2018a),

删除了: Typically, workshop waste gases are routed through collection devices, followed by collection and treatment in ROG treatment devices, before being released into the atmosphere via exhaust stacks. ROG treatment devices are implemented to reduce ROG emissions after treatment, thereby ensuring that the ROG concentrations after treatment are generally lower than those before treatment.

删除了: after treatment

371 emphasizing that raw chemicals used during the industrial activities play crucial roles
372 in determining the constituents of the industrial VCP emissions.

373 **B. Plastic surface coating industry**

374 Significant variations in ROG concentrations were also observed from the plastic
375 surface coating industry (Fig. 1b). These variations could be attributed to different
376 manufacturing process conditions and the use of different chemicals in workshops as
377 well. As shown in Fig. 2b, OVOCs contribute significantly to emissions from this
378 industry. Representative OVOCs for $C_xH_yO_1$ ions consist of isopropanol, acetone,
379 formaldehyde, methanol, and cyclohexanone. $C_xH_yO_2$ ions refer to acetates and
380 acrylates such as $C_3H_6O_2$ (e.g. methyl acetate), $C_6H_{12}O_2$ (e.g. butyl acetate), $C_9H_{16}O_2$
381 (e.g. allyl hexanoate) and $C_{12}H_{20}O_2$ (e.g. linalyl acetate). Notably, there are some
382 differences from the main components compared to previous results (Zhong et al.,
383 2017), which may be attributed to the substitution of solvent-borne chemicals with
384 water-borne chemicals in industrial VCPs.

385 **C. Furniture coating industry**

386 Due to the wide variety of industrial coatings used in the furniture coating
387 industry, numerous ROGs can be observed in the measured mass spectra (Fig. 2c).
388 Notably, $C_xH_yO_2$ (24%) and $C_xH_yO_3$ ions (9%) contribute significantly in this industry.
389 Among the identified species, C_8 aromatics exhibit the highest concentrations,
390 consistent with previous research from industries utilizing solvent-borne coatings (Yuan
391 et al., 2010; Wu et al., 2020b; Wang et al., 2014). Other OVOCs such as MEK, ethanol,
392 and formaldehyde for $C_xH_yO_1$ ions, $C_6H_{12}O_2$ (e.g. butyl acetate), $C_3H_8O_2$ (e.g. methyl
393 methacrylate, acetylacetone) for $C_xH_yO_2$ ions, and $C_6H_{12}O_3$ (e.g. propylene glycol
394 methyl ether acetate, PGMEA) and $C_7H_{14}O_3$ (e.g. butyl lactate) for $C_xH_yO_3$ ions had
395 been found may be associated with emissions from water-borne coatings. This finding
396 underscores the importance of considering high-molecular-weight OVOCs in this
397 industry, further emphasizing the ability of PTR-ToF-MS to better characterize these
398 important OVOCs that serve as raw chemicals for industrial VCPs.

399 Moreover, by employing online PTR-ToF-MS technology, we can gain deeper

删除了: Moreover, the utilization of PTR-ToF-MS enabled the identification of additional important OVOCs, thereby improving the characterization of ROG emissions from the industrial VCPs....

404 insights into the emission characteristics of ROGs during both working and non-
405 working hours. We conducted an analysis of ROG emissions in the furniture coating
406 factory during non-working hours (from 10:00 p.m. to 8:00 a.m. the next day) and
407 compared them with emissions during working hours (Fig. 1c). Most ROGs exhibited
408 a gradual decrease in concentration during non-working hours, with the exception of
409 formaldehyde which maintained a constant concentration. Notably, the concentrations
410 of other typical ROGs, such as MEK and C₈ aromatics, were 2-5 times lower during
411 non-working hours compared to working hours. This observation suggests that ROGs
412 may still be emitted even when the painting activities in the factory is halted, with night-
413 time emissions accounting for approximately 20% of total daily emissions. The θ angles
414 of mass spectra between real-time concentrations versus working hours shows that
415 ROG emissions have many similarities during both working and non-working hours
416 (Fig. 1d, $\theta < 30^\circ$ in most times). Additionally, the poor similarity observed between real-
417 time concentrations in workshops during non-working hours and those in the outside
418 air suggests that outside air has minimal influence on ROG emissions during non-
419 working hours (Fig. S8). Given that some ROGs were still more abundant and
420 continued to be released into the atmosphere even during non-working hours (e.g. from
421 the volatilization of chemicals), the ROG emissions in factories during non-working
422 hours should not be ignored.

423 **D. Printing industry**

424 The real-time concentrations of typical ROGs measured from the printing
425 industry is shown in Fig. S6a, with an emphasize on the performance of two different
426 ROG treatment devices, namely activated carbon adsorption combined with ultraviolet-
427 ray (UV) photolysis devices and catalytic combustion devices (specifically,
428 regenerative thermal oxidizer (RTO) devices) installed in this factory. Isopropanol was
429 found to have the highest concentration in the printing industry (Fig. 2d), which is
430 consistent with previous studies (Zheng et al., 2013). The higher concentrations of other
431 typical species, such as C₄H₈O₂ (e.g. ethyl acetate), C₅H₁₀O₂ (e.g. isopropyl acetate),
432 and C₇H₁₆O₃ (e.g. dipropylene glycol methyl ether, DPM) substantiate the correlation

删除了: are

434 between ROG emissions and industrial inks utilized in the printing industry. It was
435 found that ROG treatment devices exhibit varying treatment efficiencies for ROGs,
436 particularly for OVOCs (such as isopropanol and ethanol), that may not have been
437 effectively removed by these treatment devices.

438 E. Ship coating industry

439 In comparison to other industrial VCP sources, the ship coating industry exhibits
440 the highest emissions of hydrocarbons (86%), specifically C₆-C₁₁ aromatics (Fig. 2e,
441 also in Fig. S6b, Sect. S1). This may be attributed to the utilization of solvent-borne
442 industrial coatings for ship coating remains prevalent due to stringent requirements for
443 anti-rust and anti-corrosion properties (Malherbe and Mandin, 2007). A few OVOCs,
444 such as methanol and MEK, were identified as significant emissions. These results
445 confirm that ROG emissions from solvent-borne coatings, predominantly composed of
446 C₈ aromatics, continue to be the primary contributors in the ship coating industry, which
447 is consistent with a previous study conducted in the PRD region (Zhong et al., 2017).

448 3.1.2 Comparison of ROG composition from industrial VCP sources

449 The quantification of the proportions of different ion categories measured by the
450 PTR-ToF-MS across various industrial VCP sources is shown in Fig.2 and Fig. S9,
451 OVOCs make up the largest fractions in the printing (94%), plastic surface coating
452 (90%), shoemaking (84%), and furniture coating (68%) industries, while they only
453 account for 13% of emissions from the ship coating industry. The fractions of different
454 OVOC groups exhibit a general decline from C_xH_yO₁ to C_xH_yO_{≥3}, and OVOCs with
455 more than two oxygen atoms are present in small proportions (0.3%-8.5%) in all
456 industrial VCP sources except for the furniture coating industry (33%), indicating little
457 emissions of these species. However, although these OVOCs with two or more oxygen
458 atoms do not contribute significantly to the overall emissions, some of them may serve
459 as tracer compounds for particular emission sources as they were only detected in single
460 source. Previous studies have identified octamethylcyclotetrasiloxane (D₄ siloxane),
461 texanol (C₁₂H₂₄O₃) and para-chlorobenzotrifluoride (PCBTF, C₇H₄ClF₃) as tracer
462 compounds for individual chemicals (adhesives and coatings) in U.S. cities (Gkatzelis

删除了: Fig. 2 provides a

删除了: quantified

删除了:

删除了: as well

删除了:

468 et al., 2021a). We also observed that the concentrations of texanol and PCBTF emitted
469 by relevant industrial VCP sources were unique and almost non-existent in other
470 sources. Texanol was only detected in samples from the plastic surface coating and
471 furniture coating industries that utilize water-borne coatings. Similarly, PCBTF was
472 only found in samples from the ship coating and furniture coating industries that use
473 solvent-borne coatings. These findings suggest that texanol and PCBTF may be
474 applicable as tracer compounds for industrial VCPs in China. On the contrary, D₄
475 siloxane was not found to be specific to emissions from adhesive-related industrial (i.e.
476 shoemaking industry) (Fig. 2), indicating that D₄ siloxane may not be an appropriate
477 tracer compounds for identifying industrial VCPs in China.

删除了: 1

478 **3.2 Distributions of ROG emissions, OHR, OFP, and volatility**

479 We compared the mass spectra of these industrial VCP sources and calculating
480 the θ angles similarity (Fig. 3) (Table. S7). The ROG_s showed a diverse similarity
481 among different types of industrial VCP sources. Only plastic surface coating industry
482 versus printing industry demonstrated good consistency (27°), other mass spectra
483 exhibited poor consistency ($\theta > 60^\circ$). Combined with mass spectra of vehicular
484 emissions (Wang et al., 2022), the θ angle similarities among the mass spectra of
485 industrial VCP sources (62°-90°) were worse than those of vehicular emissions (41°-
486 75°) (Fig. 3). It is interesting to observe that the θ angle similarity among the mass
487 spectra in different workshops in printing and ship coating industries ranged from 1.6°
488 to 9.0° (Table. S8), similar to the mass spectra in various emission standards for
489 gasoline vehicles (4.9°-17°) (Table. S9). Conversely, the θ angle similarity among the
490 mass spectra of workshops in other industrial VCP sources ranged from 13° to 60°,
491 indicating significant differences in ROG emissions from industrial VCP sources. These
492 substantial differences indicate that ROG emissions from industrial VCPs are more
493 complex and diverse than vehicular emissions. Consequently, a more accurate
494 classification of industrial VCP emissions is necessary, as they cannot be directly
495 unified as a single class of emission sources.

删除了: 6

删除了: 7

删除了: 8

496 The combination of PTR-ToF-MS and canister-GC-MS/FID measurements

501 allowed for more comprehensive speciation of ROG emissions from industrial VCP
502 sources. This comprehensive approach enabled the determination of the fractions of
503 ROGs in total ROG emissions for various industrial VCP sources (Table. S10, Fig. S5,
504 details in Sect. S2 in the Supplement). Additionally, ROGs reactivity plays a crucial
505 role in characterizing the contributions of different ROGs to atmospheric chemical
506 reactions and the formation of secondary pollutants (Wu et al., 2020a; Yang et al., 2016).
507 The overall OHR of ROGs was calculated to comprehend the role of ROGs emitted by
508 industrial VCP sources. The calculation only employed ROGs with known reaction rate
509 constants with the OH radical, which were taken from previous studies (Atkinson and
510 Arey, 2003; Atkinson et al., 2004; Atkinson et al., 2006; Koss et al., 2018; Wu et al.,
511 2020a; Zhao et al., 2016). The fractions of ROGs in the total OHR of ROGs can be
512 determined for various industrial VCP sources (Table. S11). ROGs are grouped into
513 categories, including OVOCs, N/S-containing, and heavy aromatics and monoterpenes
514 measured by H₃O⁺ PTR-ToF-MS, higher alkanes (including C₁₀-C₂₀ acyclic, cyclic, and
515 bicyclic cycloalkanes) measured by NO⁺ PTR-ToF-MS, and alkanes, alkenes, aromatics,
516 and halohydrocarbons measured by canister-GC-MS/FID.

517 OVOCs contributed significantly to total ROG emissions (Fig. 4a), and fractions
518 of OVOCs in total ROG emissions are comparable to previous studies (Fig. 5). Notably,
519 OVOCs account for 67% of total ROG emissions from the shoemaking industry, which
520 is slightly lower than findings from other studies in the PRD region (Zheng et al., 2013)
521 but higher than those reported in previous studies (Zhou et al., 2020a; Zhao et al., 2018a).
522 The fractions of OVOCs in total ROG emissions from plastic surface coating, printing,
523 and furniture coating industries are 96%±0.2%, 85%±6.5%, and 77%, respectively.
524 Compared to previous studies (Zhong et al., 2017; Zheng et al., 2013; Fang et al.,
525 2019; Zhao et al., 2018a; Wang et al., 2019; Zhou et al., 2020a; Zhao et al., 2021),
526 determined OVOC fractions for these industrial VCP sources are much higher (Fig. 5),
527 which may be related to two reasons: (1) more OVOC species are detected in this study;
528 (2) water-borne coatings and inks are more widely employed in the recent year which
529 may enhance OVOC fractions. Moreover, OVOCs account for 16%±3.5% of total ROG

删除了: 9

删除了: 10

532 emissions from the ship coating industry by using the solvent-borne coatings, and the
533 fraction is also higher than findings from ~~one previous study~~ (Zhong et al., 2017).
534 Additionally, OVOCs also contribute to the largest fraction in total OHR of ROGs from
535 all industrial VCP sources (72%-97%) except for the ship coating industry (15%±3.6%)
536 (Fig. 4b). In contrast to the important contribution of OVOCs, the fractions of
537 hydrocarbons measured by canister-GC-MS/FID only made considerable contributions
538 in specific industrial VCP sources (Fig. 4). For instance, aromatics were found to be the
539 major contributors to both total ROG emissions and OHR in the ship coating industry,
540 making up 74%±6.1% and 79%±4.8% respectively. Alkanes measured by canister-GC-
541 MS/FID only make contributions in the shoemaking industry, comprising 26% of the
542 total ROG emissions. Overall, the total OHR of ROGs was dominated by OVOCs and
543 aromatics, and the contributions of other species were in the range of 1.8%-21% (Fig.
544 4b). These results stress the importance of measuring a broad range of OVOCs using
545 PTR-ToF-MS in characterizing ROG emissions from industrial VCP sources.

删除了: in

546 The application of NO⁺ PTR-ToF-MS provided the opportunity for detecting
547 emissions of higher alkanes from industrial VCP sources. We show that the contribution
548 of higher alkanes can be significant for VCP sources. Specifically, the printing industry
549 demonstrates a noteworthy presence of higher alkanes, accounting for 27%±2.7% and
550 8.2%±2.4% in workshop and stack emissions, respectively (Table. S10). This can be
551 attributed to the use of lubricating oil, a primary component of industrial inks, which
552 contains substantial amounts of alkanes (Liang et al., 2018). Furthermore, emissions
553 from forklifts transporting products in printing workshops also contribute to the
554 emission of higher alkanes (Li et al., 2021), suggesting non-road vehicles may
555 contribute to the emissions from industrial VCP factories. In addition, the fractions of
556 higher alkanes in stack emission are lower than in workshops, suggesting that ROG
557 treatment devices effectively reduce emissions of higher alkanes.

删除了: 9

558 To facilitate for making controlling strategies ~~of~~ ozone, we determine the ~~OFP~~
559 ~~from~~ a unity of emission from different sources for comparison (Yuan et al., 2010; Na
560 and Pyo Kim, 2007), which represent the ability to ozone formation from ROG sources

删除了: for

删除了: ozone formation potential for

565 on a relative basis (Fig. 6), and calculated using the following equation:

$$OFP_i = \sum_{j=1}^n f_{ji}MIR_j \quad (2)$$

567 Where OFP_i is the estimated ozone formation amount when 1 g ROG is emitted
568 from source i , f_{ji} is the mass fraction of species j in source i , and MIR_j is the
569 maximum incremental reactivity (MIR) of species j (Carter, 2007). Among the
570 industrial VCP sources considered, the ship coating industry exhibited the highest OFP,
571 reaching as high as $5.5 \text{ g O}_3 \cdot \text{g}^{-1}$ ROG, followed by the furniture coating industry, with
572 a value of $2.7 \text{ g O}_3 \cdot \text{g}^{-1}$ ROG. The OFP for other industrial VCP sources ranged from
573 $0.79 \text{ g O}_3 \cdot \text{g}^{-1}$ ROG to $1.4 \text{ g O}_3 \cdot \text{g}^{-1}$ ROG. Among all industrial VCP sources, aromatics
574 (ranging from 4.2% to 91%) and OVOCs (ranging from 6.7% to 94%) were identified
575 as the primary contributors to OFP. Compared to vehicular emissions, the OFP from the
576 ship coating and furniture coating industries are significantly higher (Fig. 6), suggesting
577 that these sources should be controlled in priority. Given the higher reactivity value for
578 ship coating industry relative to other sources, it is evident that controlling ROG
579 emissions from solvent-borne industrial chemicals would have a more substantial
580 impact on reducing ozone formation compared to other sources. Moreover, it is
581 important to note that the emissions of solvent-borne chemicals surpass those of
582 vehicles, while water-borne chemicals have lower emissions compared to vehicles. This
583 observation implies that the substitution of solvent-borne chemicals with water-borne
584 chemicals in China holds considerable importance in mitigating and controlling ozone
585 pollution.

586 We further compare centralization for species among different ROG sources by
587 determining the contribution from the top ten species in terms of concentrations, OHR,
588 and OFP (Fig. 7 and Fig. S10, also in Table S12). We show that the top ten ROG
589 account for over 50% on ROG emissions, OHR, and OFP (Fig. 7). With the exception
590 of furniture coating industry, the fractions on the top ten species in total emissions, OHR,
591 and OFP from industrial VCP sources were in range of 89%-96%. The lower fractions
592 (ranging from 69% to 86%) of the top ten species in the furniture coating industry may
593 be a result of the wider range of industrial coatings (i.e. both solvent-borne and water-

删除了: Our calculations specifically focused on ROG with known ...

删除了: values

删除了: , derived from previous studies

删除了:

删除了: 5

删除了: 8

删除了: 11

602 borne coatings) utilized in this industry. ROG emissions from industrial VCP sources are
603 apparently more centralized compared to vehicular emissions (ranging from 51% to
604 87%). Additionally, the cumulative fractions of the top one hundred species in overall
605 ROG emissions, OHR, and OFP in various industrial VCP sources is further indicated
606 the highly centralized of ROG emissions from various emission sources (Fig. S10).
607 More than half of the top ten species in ROG emissions, OHR, and OFP from industrial
608 VCP sources were OVOCs (Table S13). Among them, isopropanol made a notable
609 contribution to the printing, plastic surface coating, and shoemaking industries. Other
610 OVOCs such as MEK, acetone, and ethyl acetate contributed to total ROG emissions
611 in each industry, while formaldehyde, acetaldehyde contributed to total OHR and OFP.
612 It should be noted that the proportions of C₁₃, C₁₄, and C₁₅ cycloalkanes from printing
613 industry (account for 6.3% in ROG emissions), as well as the proportion of C₁₁
614 aromatics from ship coating industry (account for 1.0% in ROG emissions) are not
615 negligible. Additionally, acetylacetone is a common species with broad industrial
616 applications, and contributes importantly to secondary pollutants formation under
617 polluted environments (Ji et al., 2018). Although it only contributes 8.7% to total
618 emissions from the furniture coating industry, its fraction in terms of total OHR can be
619 as high as 30%. These findings demonstrated that previously underreported ROGs
620 should receive greater attention in future research.

621 The updated measurements of OVOC emissions by using the PTR-ToF-MS
622 substantially improve our understanding of the emission of industrial VCP sources. The
623 effective saturation concentrations (C*) of high-molecular-weight OVOCs were found
624 to be lower, which were corresponding to intermediate-volatility organic compounds
625 (IVOCs) and semi-volatile organic compounds (SVOCs). Since these S/I-VOCs are
626 crucial precursors for the SOA in urban environments (Zhao et al., 2014), it is important
627 to comprehend their contributions from the emissions of industrial VCP sources across
628 various volatility classes, including volatility organic compounds (VOCs), IVOCs, and
629 SVOCs (Guenther et al., 2012; Li et al., 2016). Fig. 8 illustrates the distribution of ROG
630 species in a two-dimensional volatility basis set (2D-VBS) space for various industrial

删除了: 8

删除了: 11

633 VCP sources, categorized based on volatility bins (Li et al., 2016;Donahue et al., 2011).
634 It is worth noting that the volatility distributions exhibit substantial variation across
635 industrial VCP sources (Fig. 8a). Generally, VOCs constitute the predominant fraction
636 of emissions from industrial VCP sources, accounting for 59% to 98% of the total
637 emissions. The fractions of IVOCs are largest in the printing industry (40%), compared
638 to the range of 2.1%-9.6% in other industrial VCP sources. Conversely, the contribution
639 of SVOCs from industrial VCP sources are negligible in our study, accounting for less
640 than 1%. Considering the importance of S/I-VOCs in SOA formation, particularly with
641 the increasing adoption of improved online mass spectrometry technologies, the S/I-
642 VOCs emissions from industrial VCP sources should be paid more attention in future
643 research.

644 3.3 Evaluate ROGs treatment efficiency in industrial VCP sources

645 The analysis of the PTR-ToF-MS mass spectra offers valuable insights into the
646 impact of ROG emissions from industrial VCP sources. This comprehensive
647 information provided by the PTR-ToF-MS also allows for a systematic comparison of
648 emissions before and after the treatment of ROGs. ~~The scatterplot of the concentrations~~
649 ~~of various ROGs before and after treatment in industrial VCP sources are shown in Fig.~~
650 ~~9 and Fig. S11.~~ The observed treatment efficiency, represented by 1-slope, did not reach
651 the desired levels, ranging from -12% to 68%. Among the industrial VCP sources
652 investigated, the shoemaking industry exhibited the highest treatment efficiency
653 (slope=0.32) with the activated carbon adsorption combined with UV photolysis device.
654 This remarkable efficiency can be attributed to the large-scale nature of the factory and
655 meticulous regulation of the ROG treatment devices. Following closely behind is the
656 printing industry, utilizing catalytic combustion devices, with a slightly higher efficacy
657 (slope=0.67) than another treatment device in the same factory (slope=0.80).
658 ~~Nonetheless,~~ it is evident that the treatment efficiency has not reached the desired levels
659 ~~for all ROG groups (Fig. S11), which~~ possibly due to the challenges associated with
660 effectively removing ~~majority ROG emissions using current treatment technologies.~~
661 Additionally, we also observed that some OVOCs may be generated as byproducts after

删除了: ROG treatment devices are employed to reduce ROG emissions after treatment. Here, we evaluate two types of ROG treatment devices: activated carbon adsorption combined with UV photolysis devices (installed in shoemaking, plastic surface coating, furniture coating, and printing industries) and catalytic combustion devices (installed in printing and ship coating industries).

删除了: However,

删除了: OVOC

删除了:

删除了: from the printing industry

673 the implementation of treatment devices. For instance, the concentrations of CH₂O₂ (e.g.
674 formic acids), C₄H₆O₃ (e.g. propylene carbonate), and C₉H₁₈O (e.g. nonanal) were
675 found to be higher after the application of activated carbon adsorption combined with
676 UV photolysis devices (Fig. 9d). Similarly, the concentrations of C₃H₄O (e.g. acrolein)
677 and C₁₂H₁₈O₄ (e.g. dibutyl squarate) were also higher following the utilization of
678 catalytic combustion devices (Fig. 9e). Therefore, it is crucial to consider the potential
679 contribution of these ROGs when assessing the emissions released into the atmosphere.

680 The lowest treatment efficiency of ROG was obtained in the furniture coating industry
681 (slope=1.12). This treatment device demonstrates inefficiency for all ROG groups (Fig.
682 S11). The inadequate performance of the ROG treatment devices in this specific facility
683 may be attributed to a number of possible reasons, e.g., delayed replacement of
684 activated carbon and other adsorption materials, and the implementation of the UV
685 photolysis device could potentially result in the generation of more ROGs as byproducts.

686 Furthermore, the θ angles between the mass spectra of ROG from workshops,
687 before and after ROG treatment devices for various industrial VCP sources were
688 calculated and summarized in Fig. S12 (also in Table. S13). A comparison between the
689 correlation of mass spectra among workshops versus after treatment devices (ranging
690 from 6.2° to 49°) and workshops versus before treatment devices (ranging from 4.2° to
691 41°) demonstrated a poorer correlation in the former case. The similarities between
692 workshops and stack emissions in the shoemaking industry were lower compared to
693 other industrial VCP sources. This discrepancy can potentially be attributed to the
694 inclusion of ROG emissions from non-VCP usage manufacturing processes (e.g. sole
695 injection molding) in the collection process of ROG treatment devices. Additionally,
696 the θ angles similarity between the mass spectra from before and after ROG treatment
697 devices in various industrial VCP sources also providing insight into the efficacy of the
698 devices in removing ROGs (Fig. 9). The θ angles in ROG treatment devices from five
699 industrial VCP sources were found to range from 1.8° to 27°, indicating good
700 consistency between the mass spectra before and after treatment of ROGs. This
701 alignment suggests that the chemical compositions of ROG emissions remain

删除了: in printing industry

删除了: shown

删除了: potentially attributed to the ineffective performance of the ROG treatment devices in this particular facility, as activated carbon and other adsorption materials were not promptly replaced

删除了:

删除了: 9

删除了: 12

711 comparable before and after treatment ($R \geq 0.87$), implying that the relative proportions
712 of various ROG components are not significantly affected by the ROG treatment
713 devices in these industrial VCP sources.

714 **3.4 Impact of industrial VCP sources on ambient air**

715 To gain deeper insights into the atmospheric impact of emissions from industrial
716 VCP sources, an in-situ measurement was carried out at a monitoring station nearby the
717 furniture coating industry, located 2 km northeast from the industry site. The
718 measurement was conducted using a PTR-ToF-MS (Kore Inc., U.K.), which enabled
719 the quantification of various common ROGs. More information about this instrument
720 and dataset for in-situ measurement can be found elsewhere (Gonzalez-Mendez et al.,
721 2016; Song et al., 2023). Concordant with expectations, the average concentrations of
722 representative ROGs generally demonstrate a discernible decline from the furniture
723 coating industry (including stack emission and workshops during working and non-
724 working hours) to the ambient measurement (Fig. 10). C₈ aromatics and MEK
725 performed considerable emissions from furniture coating industry, while the
726 concentrations of them in the ambient air are orders of magnitude lower than those
727 observed in the industry. However, ambient concentrations of OVOCs, specifically
728 MEK (6.8 ± 8.2 ppb) and ethyl acetate (7.5 ± 5.9 ppb) are still significantly higher than
729 clean environments and are among the highest measured concentration in the literature
730 (Wu et al., 2020a; He et al., 2022b; Khare et al., 2022; Yang et al., 2022). It is confirmed
731 that OVOCs should be paid attention to industrialized urban areas, thereby further
732 substantiating the significance of OVOC emissions from industrial VCP sources to
733 atmospheric pollution. These results stress the invaluable insights provided by PTR-
734 ToF-MS in comprehensively characterizing ROG compositions in both emission
735 sources and urban air.

736 The preceding discussions illustrate that the emission characteristics of ROGs
737 significantly vary among industrial VCP sources. As a result, the ratio of ROG pairs
738 can be used to distinguish emissions of industrial VCP sources. MEK and C₈ aromatics
739 emerge as key species in industrial VCP emissions, and the reaction rate constants of

删除了: Comparison

删除了: and

删除了: monitor station

删除了:

删除了: in

745 C₈ aromatics with OH radical ($k_{OH} = (1.4-2.3) \times 10^{-11} \text{ cm}^3 \cdot \text{molecule}^{-1} \cdot \text{s}^{-1}$) are higher
746 than MEK ($k_{OH} = 5.5 \times 10^{-12} \text{ cm}^3 \cdot \text{molecule}^{-1} \cdot \text{s}^{-1}$) (Atkinson and Arey, 2003; Wu et al.,
747 2020a). Fig. 11 illustrates the correlation of MEK with C₈ aromatics in stack emission,
748 workshops during working hours and non-working hours in the furniture coating
749 industry, as well as ambient measurement near the industry. Positive correlations
750 between MEK and C₈ aromatics are observed in both emission sources and ambient
751 measurements, indicating a shared source for these compounds. Additionally, the
752 observed ratios of MEK to C₈ aromatics in ambient measurement are also comparable
753 with the ratios of MEK to C₈ aromatics measured in emissions from the furniture
754 coating industry (0.97 ppb·ppb⁻¹ for the stack emission and 0.75 ppb·ppb⁻¹ for the
755 workshops emission), suggesting that industrial VCP emissions (specifically furniture
756 coating) may account for the enhancement of MEK and C₈ aromatics in this industrial
757 area. The peak concentration of MEK exceeding 200 ppb from the ambient
758 measurements are among the highest in the literature (Fig. 11). Therefore, we conducted
759 a comparison of MEK and C₈ aromatics concentrations in this study with those in clean
760 environments (urban, rural, forest, and coastal sites) from previous studies (Fig. S13)
761 (Wu et al., 2020a; Coggon et al., 2024; Yuan et al., 2012; Seco et al., 2011; Acton et al.,
762 2016; Tan et al., 2021; He et al., 2022b). It is indicating that ambient measurements in
763 industrial areas have been significantly impacted by industrial VCP sources, and the
764 MEK / C₈ aromatics ratio can serve as good evidence by using high time-resolution
765 ROG measurements from PTR-ToF-MS.

删除了: C8

766 4. Conclusion

767 In this work, we conducted a field campaign to measure more comprehensive
768 speciation of ROG emissions from industrial VCP sources, including shoemaking,
769 plastic surface coating, furniture coating, printing, and ship coating industries. To
770 achieve this, we employed the PTR-ToF-MS in combination with canister-GC-MS/FID
771 techniques. Our study demonstrated that OVOCs have been identified as representative
772 ROGs emitted from these sources, which are highly related to specific chemicals used
773 during the industrial activities. Furthermore, we performed a mass spectra similarity

删除了:

Thus, the divergence in MEK / C₈ aromatics ratio among different industrial VCP sources suggests that these ratios could serve as effective indicators for distinguishing industrial VCP emissions, particularly in ambient measurements within industrial areas. Consequently, the MEK to C₈ aromatics ratio could provide an additional tracer for assessing the contribution of industrial VCP emissions by using high time-resolution ROG measurements from PTR-ToF-MS....

删除了: identified

删除了: had

787 analysis to compare the ROG emissions across different emission sources. The poor
788 consistency of the similarity between the mass spectra in emission sources indicating
789 that substantial differences between industrial VCP sources, as they cannot be directly
790 categorized as a single class of emission sources.

791 In addition, the fractions of ROGs in total ROG emissions and OHR are
792 determined by combining measurements from canister-GC-MS/FID and PTR-ToF-MS.
793 Except for the ship coating industry utilizing solvent-borne coatings, the proportions of
794 OVOCs range from 67% to 96% in total ROG emissions and 72% to 97% in total OHR
795 for different industrial sources. Large fraction of OVOCs may be related to two reasons:
796 (1) more OVOC species are detected in this study; (2) water-borne coatings and inks
797 are more widely employed in the recent year which may enhance OVOC fractions. This
798 highlights the importance of measuring these OVOC emissions from industrial VCP
799 sources. The industrial VCP sources associated with solvent-borne coatings exhibited a
800 higher OFP, reaching as high as 5.5 and 2.7 g O₃:g⁻¹ ROGs for ship coating and
801 furniture coating industries, primarily due to contributions from aromatics, suggesting
802 that these sources should be controlled in priority. The fractions of the ten most
803 abundant species in total ROG emissions, OHR, and OFP indicate the highly centralized
804 of ROG emissions from various emission sources.

805 Our results suggest that ROG treatment devices may have limited effectiveness
806 in removing ROGs, with treatment efficiencies ranging from -12% to 68%. In addition,
807 OVOCs should be paid more attention to industrialized urban areas due to the
808 substantial impact of industrial VCP sources. Our study demonstrated that ROG pairs
809 (e.g., MEK / C₈ aromatics ratio) can be utilized as reliable evidence for indicating the
810 impact of industrial VCP sources on ambient measurements in industrial areas.

811 This study highlights the significant role of OVOCs to ROG emissions from
812 industrial VCP sources, particularly those utilizing water-borne chemicals. As a result,
813 these industrial VCP sources may significantly contribute to the primary emissions of
814 OVOCs in urban regions. The current emission inventories do not fully account for the
815 emissions of many ROGs, which can compromise the predictive accuracy of air quality

删除了: the average concentrations of representative ROGs generally demonstrate a downward trend from emission sources to the ambient air. Our results demonstrate that

删除了:

删除了: indicators for distinguishing industrial VCP sources, particularly for measurements in industrial areas

822 models in urban areas. In this study, a broader range of ROG species was quantified
823 using PTR-ToF-MS measurements, which highlights the effectiveness of PTR-ToF-MS
824 in characterizing ROG emissions from industrial VCP sources.

删除了:.

826 **Data availability**

827 Data are available from the authors upon request.

828 **Author contribution**

829 BY designed the research. BY and SHW organized industrial VCP source
830 measurements. SHW, XJH, RC, CHW, and CMW contributed to data collection. SHW
831 performed the data analysis, with contributions from XS and YBC. SHW and BY
832 prepared the manuscript with contributions from YBH, XBL, BGW and MS. All the
833 authors reviewed the manuscript.

834 **Competing interests**

835 The authors declare that they have no known competing financial interests or
836 personal relationships that could have appeared to influence the work reported in this
837 paper.

838 **Acknowledgement**

839 This work was supported by the National Key R&D Plan of China (grant No.
840 2022YFC3700604), the National Natural Science Foundation of China (grant No.
841 42230701, and 42205094). This work was also Supported by the Outstanding
842 Innovative Talents Cultivation Funded Programs for Doctoral Students of Jinan
843 University (grant No.2022CXB028).

844

846 **References**

- 847 Acton, W. J. F., Schallhart, S., Langford, B., Valach, A., Rantala, P., Fares, S., Carriero,
848 G., Tillmann, R., Tomlinson, S. J., Dragosits, U., Gianelle, D., Hewitt, C. N., and
849 Nemitz, E.: Canopy-scale flux measurements and bottom-up emission estimates of
850 volatile organic compounds from a mixed oak and hornbeam forest in northern Italy,
851 *Atmospheric Chemistry and Physics*, 16, 7149-7170, 10.5194/acp-16-7149-2016, 2016.
852 Atkinson, R., and Arey, J.: Atmospheric Degradation of Volatile Organic Compounds,
853 *Chemical Reviews*, 103, 4605-4638, 10.1021/cr0206420, 2003.
854 Atkinson, R., Baulch, D. L., Cox, R. A., Crowley, J. N., Hampson, R. F., Hynes, R. G.,
855 Jenkin, M. E., Rossi, M. J., and Troe, J.: Evaluated kinetic and photochemical data for
856 atmospheric chemistry: Volume I - gas phase reactions of Ox, HOx, NOx and SOx
857 species, *Atmos. Chem. Phys.*, 4, 1461-1738, 10.5194/acp-4-1461-2004, 2004.
858 Atkinson, R., Baulch, D. L., Cox, R. A., Crowley, J. N., Hampson, R. F., Hynes, R. G.,
859 Jenkin, M. E., Rossi, M. J., Troe, J., and Subcommittee, I.: Evaluated kinetic and
860 photochemical data for atmospheric chemistry: Volume II – gas phase reactions
861 of organic species, *Atmos. Chem. Phys.*, 6, 3625-4055, 10.5194/acp-6-3625-2006, 2006.
862 Buhr, K., van Ruth, S., and Delahunty, C.: Analysis of volatile flavour compounds by
863 Proton Transfer Reaction-Mass Spectrometry: fragmentation patterns and
864 discrimination between isobaric and isomeric compounds, *International Journal of*
865 *Mass Spectrometry*, 221, 1-7, [https://doi.org/10.1016/S1387-3806\(02\)00896-5](https://doi.org/10.1016/S1387-3806(02)00896-5), 2002.
866 Cappellin, L., Karl, T., Probst, M., Ismailova, O., Winkler, P. M., Soukoulis, C., Aprea,
867 E., Mark, T. D., Gasperi, F., and Biasioli, F.: On quantitative determination of volatile
868 organic compound concentrations using proton transfer reaction time-of-flight mass
869 spectrometry, *Environmental Science & Technology*, 46, 2283-2290,
870 10.1021/es203985t, 2012.
871 Carter, W. P.: Development of the SAPRC-07 chemical mechanism and updated ozone
872 reactivity scales, Citeseer, 2007.
873 Chang, X., Zhao, B., Zheng, H., Wang, S., Cai, S., Guo, F., Gui, P., Huang, G., Wu, D.,
874 Han, L., Xing, J., Man, H., Hu, R., Liang, C., Xu, Q., Qiu, X., Ding, D., Liu, K., Han,
875 R., Robinson, A. L., and Donahue, N. M.: Full-volatility emission framework corrects
876 missing and underestimated secondary organic aerosol sources, *One Earth*, 5, 403-412,
877 <https://doi.org/10.1016/j.oneear.2022.03.015>, 2022.
878 Chen, Y., Yuan, B., Wang, C., Wang, S., He, X., Wu, C., Song, X., Huangfu, Y., Li, X.
879 B., Liao, Y., and Shao, M.: Online measurements of cycloalkanes based on NO⁺
880 chemical ionization in proton transfer reaction time-of-flight mass spectrometry (PTR-
881 ToF-MS), *Atmos. Meas. Tech.*, 15, 6935-6947, 10.5194/amt-15-6935-2022, 2022.
882 Coggon, M. M., McDonald, B. C., Vlasenko, A., Veres, P. R., Bernard, F., Koss, A. R.,
883 Yuan, B., Gilman, J. B., Peischl, J., Aikin, K. C., DuRant, J., Warneke, C., Li, S. M.,
884 and de Gouw, J. A.: Diurnal Variability and Emission Pattern of
885 Decamethylcyclopentasiloxane (D5) from the Application of Personal Care Products in
886 Two North American Cities, *Environ Sci Technol*, 52, 5610-5618,
887 10.1021/acs.est.8b00506, 2018.

888 Coggon, M. M., Gkatzelis, G. I., McDonald, B. C., Gilman, J. B., Schwantes, R. H.,
889 Abuhassan, N., Aikin, K. C., Arend, M. F., Berkoff, T. A., Brown, S. S., Campos, T. L.,
890 Dickerson, R. R., Gronoff, G., Hurley, J. F., Isaacman-VanWertz, G., Koss, A. R., Li,
891 M., McKeen, S. A., Moshary, F., Peischl, J., Pospisilova, V., Ren, X., Wilson, A., Wu,
892 Y., Trainer, M., and Warneke, C.: Volatile chemical product emissions enhance ozone
893 and modulate urban chemistry, *Proc Natl Acad Sci U S A*, 118,
894 10.1073/pnas.2026653118, 2021.

895 Coggon, M. M., Stockwell, C. E., Clafin, M. S., Pfannerstill, E. Y., Xu, L., Gilman, J.
896 B., Marcantonio, J., Cao, C., Bates, K., Gkatzelis, G. I., Lamplugh, A., Katz, E. F., Arata,
897 C., Apel, E. C., Hornbrook, R. S., Piel, F., Majluf, F., Blake, D. R., Wisthaler, A.,
898 Canagaratna, M., Lerner, B. M., Goldstein, A. H., Mak, J. E., and Warneke, C.:
899 Identifying and correcting interferences to PTR-ToF-MS measurements of isoprene and
900 other urban volatile organic compounds, *Atmospheric Measurement Techniques*, 17,
901 801-825, 10.5194/amt-17-801-2024, 2024.

902 de Gouw, J., and Warneke, C.: Measurements of volatile organic compounds in the
903 earth's atmosphere using proton-transfer-reaction mass spectrometry, *Mass Spectrom*
904 *Rev* 26, 223-257, 10.1002/mas.20119, 2007.

905 Donahue, N. M., Epstein, S. A., Pandis, S. N., and Robinson, A. L.: A two-dimensional
906 volatility basis set: 1. organic-aerosol mixing thermodynamics, *Atmospheric Chemistry*
907 *and Physics*, 11, 3303-3318, 10.5194/acp-11-3303-2011, 2011.

908 Fang, L., Liu, W., Chen, D., Li, G., Wang, D., Shao, X., and Nie, L.: Source Profiles of
909 Volatile Organic Compounds (VOCs) from Typical Solventbased Industries in Beijing
910 (in Chinese), *Environmental Science*, 40, 4395-4403, 10.13227/j.hjcx.201901128,
911 2019.

912 Fortner, E. C., Zheng, J., Zhang, R., Berk Knighton, W., Volkamer, R. M., Sheehy, P.,
913 Molina, L., and André, M.: Measurements of Volatile Organic Compounds Using
914 Proton Transfer Reaction – Mass Spectrometry during the MILAGRO 2006 Campaign,
915 *Atmos. Chem. Phys.*, 9, 467-481, 10.5194/acp-9-467-2009, 2009.

916 Gao, Y., Wang, H., Yuan, L., Jing, S., Yuan, B., Shen, G., Zhu, L., Koss, A., Li, Y., Wang,
917 Q., Huang, D. D., Zhu, S., Tao, S., Lou, S., and Huang, C.: Measurement report:
918 Underestimated reactive organic gases from residential combustion – insights from a
919 near-complete speciation, *Atmospheric Chemistry and Physics*, 23, 6633-6646,
920 10.5194/acp-23-6633-2023, 2023.

921 Gkatzelis, G. I., Coggon, M. M., McDonald, B. C., Peischl, J., Aikin, K. C., Gilman, J.
922 B., Trainer, M., and Warneke, C.: Identifying Volatile Chemical Product Tracer
923 Compounds in U.S. Cities, *Environ Sci Technol*, 55, 188-199, 10.1021/acs.est.0c05467,
924 2021a.

925 Gkatzelis, G. I., Coggon, M. M., McDonald, B. C., Peischl, J., Gilman, J. B., Aikin, K.
926 C., Robinson, M. A., Canonaco, F., Prevot, A. S. H., Trainer, M., and Warneke, C.:
927 Observations Confirm that Volatile Chemical Products Are a Major Source of
928 Petrochemical Emissions in U.S. Cities, *Environ Sci Technol*, 55, 4332-4343,
929 10.1021/acs.est.0c05471, 2021b.

930 Gonzalez-Mendez, R., Watts, P., Olivenza-Leon, D., Reich, D. F., Mullock, S. J., Corlett,
931 C. A., Cairns, S., Hickey, P., Brookes, M., and Mayhew, C. A.: Enhancement of

932 Compound Selectivity Using a Radio Frequency Ion-Funnel Proton Transfer Reaction
933 Mass Spectrometer: Improved Specificity for Explosive Compounds, *Anal Chem*, 88,
934 10624-10630, 10.1021/acs.analchem.6b02982, 2016.

935 Guenther, A. B., Jiang, X., Heald, C. L., Sakulyanontvittaya, T., Duhl, T., Emmons, L.
936 K., and Wang, X.: The Model of Emissions of Gases and Aerosols from Nature version
937 2.1 (MEGAN2.1): an extended and updated framework for modeling biogenic
938 emissions, *Geoscientific Model Development*, 5, 1471-1492, 10.5194/gmd-5-1471-
939 2012, 2012.

940 Haase, K. B., Keene, W. C., Pszenny, A. A. P., Mayne, H. R., Talbot, R. W., and Sive,
941 B. C.: Calibration and intercomparison of acetic acid measurements using proton-
942 transfer-reaction mass spectrometry (PTR-MS), *Atmospheric Measurement Techniques*,
943 5, 2739-2750, 10.5194/amt-5-2739-2012, 2012.

944 Han, C., Liu, R., Luo, H., Li, G., Ma, S., Chen, J., and An, T.: Pollution profiles of
945 volatile organic compounds from different urban functional areas in Guangzhou China
946 based on GC/MS and PTR-TOF-MS: Atmospheric environmental implications,
947 *Atmospheric Environment*, 214, 10.1016/j.atmosenv.2019.116843, 2019.

948 He, X., Che, X., Gao, S., Chen, X., Pan, M., Jiang, M., Zhang, S., Jia, H., and Duan, Y.:
949 Volatile organic compounds emission inventory of organic chemical raw material
950 industry, *Atmospheric Pollution Research*, 13, 10.1016/j.apr.2021.101276, 2022a.

951 He, X., Yuan, B., Wu, C., Wang, S., Wang, C., Huangfu, Y., Qi, J., Ma, N., Xu, W.,
952 Wang, M., Chen, W., Su, H., Cheng, Y., and Shao, M.: Volatile organic compounds in
953 wintertime North China Plain: Insights from measurements of proton transfer reaction
954 time-of-flight mass spectrometer (PTR-ToF-MS), *Journal of Environmental Sciences*,
955 10.1016/j.jes.2021.08.010, 2022b.

956 Huang, C., Chen, C. H., Li, L., Cheng, Z., Wang, H. L., Huang, H. Y., Streets, D. G.,
957 Wang, Y. J., Zhang, G. F., and Chen, Y. R.: Emission inventory of anthropogenic air
958 pollutants and VOC species in the Yangtze River Delta region, China, *Atmospheric*
959 *Chemistry and Physics*, 11, 4105-4120, 10.5194/acp-11-4105-2011, 2011.

960 Huangfu, Y., Yuan, B., Wang, S., Wu, C., He, X., Qi, J., de Gouw, J., Warneke, C.,
961 Gilman, J. B., Wisthaler, A., Karl, T., Graus, M., Jobson, B. T., and Shao, M.: Revisiting
962 Acetonitrile as Tracer of Biomass Burning in Anthropogenic-Influenced Environments,
963 *Geophysical Research Letters*, 48, 10.1029/2020gl092322, 2021.

964 Humes, M. B., Wang, M., Kim, S., Machesky, J. E., Gentner, D. R., Robinson, A. L.,
965 Donahue, N. M., and Presto, A. A.: Limited Secondary Organic Aerosol Production
966 from Acyclic Oxygenated Volatile Chemical Products, *Environ Sci Technol*, 56, 4806-
967 4815, 10.1021/acs.est.1c07354, 2022.

968 Inomata, S., Tanimoto, H., and Yamada, H.: Mass Spectrometric Detection of Alkanes
969 Using NO⁺ Chemical Ionization in Proton-transfer-reaction Plus Switchable Reagent
970 Ion Mass Spectrometry, *Chemistry Letters*, 43, 538-540, 10.1246/cl.131105, 2014.

971 Ji, Y., Zheng, J., Qin, D., Li, Y., Gao, Y., Yao, M., Chen, X., Li, G., An, T., and Zhang,
972 R.: OH-Initiated Oxidation of Acetylacetone: Implications for Ozone and Secondary
973 Organic Aerosol Formation, *Environ Sci Technol*, 52, 11169-11177,
974 10.1021/acs.est.8b03972, 2018.

975 Kamal, M. S., Razzak, S. A., and Hossain, M. M.: Catalytic oxidation of volatile organic
976 compounds (VOCs) – A review, *Atmospheric Environment*, 140, 117-134,
977 10.1016/j.atmosenv.2016.05.031, 2016.

978 Khare, P., and Gentner, D. R.: Considering the future of anthropogenic gas-phase
979 organic compound emissions and the increasing influence of non-combustion sources
980 on urban air quality, *Atmospheric Chemistry and Physics*, 18, 5391-5413, 10.5194/acp-
981 18-5391-2018, 2018.

982 Khare, P., Krechmer, J. E., Machesky, J. E., Hass-Mitchell, T., Cao, C., Wang, J., Majluf,
983 F., Lopez-Hilfiker, F., Malek, S., Wang, W., Seltzer, K., Pye, H. O. T., Commane, R.,
984 McDonald, B. C., Toledo-Crow, R., Mak, J. E., and Gentner, D. R.: Ammonium adduct
985 chemical ionization to investigate anthropogenic oxygenated gas-phase organic
986 compounds in urban air, *Atmospheric Chemistry and Physics*, 22, 14377-14399,
987 10.5194/acp-22-14377-2022, 2022.

988 Koss, A. R., Warneke, C., Yuan, B., Coggon, M. M., Veres, P. R., and de Gouw, J. A.:
989 Evaluation of NO⁺ reagent ion chemistry for online measurements of atmospheric
990 volatile organic compounds, *Atmospheric Measurement Techniques*, 9, 2909-2925,
991 10.5194/amt-9-2909-2016, 2016.

992 Koss, A. R., Sekimoto, K., Gilman, J. B., Selimovic, V., Coggon, M. M., Zarzana, K.
993 J., Yuan, B., Lerner, B. M., Brown, S. S., Jimenez, J. L., Krechmer, J., Roberts, J. M.,
994 Warneke, C., Yokelson, R. J., and de Gouw, J.: Non-methane organic gas emissions
995 from biomass burning: identification, quantification, and emission factors from PTR-
996 ToF during the FIREX 2016 laboratory experiment, *Atmospheric Chemistry and
997 Physics*, 18, 3299-3319, 10.5194/acp-18-3299-2018, 2018.

998 Kostenidou, E., Lee, B.-H., Engelhart, G. J., Pierce, J. R., and Pandis, S. N.: Mass
999 Spectra Deconvolution of Low, Medium, and High Volatility Biogenic Secondary
1000 Organic Aerosol, *Environmental Science & Technology*, 43, 4884-4889,
1001 10.1021/es803676g, 2009.

1002 Li, C., Cui, M., Zheng, J., Chen, Y., Liu, J., Ou, J., Tang, M., Sha, Q., Yu, F., Liao, S.,
1003 Zhu, M., Wang, J., Yao, N., and Li, C.: Variability in real-world emissions and fuel
1004 consumption by diesel construction vehicles and policy implications, *Sci Total Environ*,
1005 786, 147256, 10.1016/j.scitotenv.2021.147256, 2021.

1006 Li, G., Jiang, B., Wang, S., Li, C., Yuan, B., Wang, B., and Zhanyi, Z.: Determination
1007 of 118 Volatile Organic Compounds in Source Emission by Canister Sampling-
1008 Preconcentration /Gas Chromatography – Mass Spectrometry (in Chinese), *Journal of
1009 Instrumental Analysis*, 39, 1441-1450, 2020.

1010 Li, L., and Cocker, D. R.: Molecular structure impacts on secondary organic aerosol
1011 formation from glycol ethers, *Atmospheric Environment*, 180, 206-215,
1012 10.1016/j.atmosenv.2017.12.025, 2018.

1013 Li, M., Zhang, Q., Zheng, B., Tong, D., Lei, Y., Liu, F., Hong, C. P., Kang, S. C., Yan,
1014 L., Zhang, Y. X., Bo, Y., Su, H., Cheng, Y. F., and He, K. B.: Persistent growth of
1015 anthropogenic non-methane volatile organic compound (NMVOC) emissions in China
1016 during 1990–2017: drivers, speciation and ozone formation potential, *Atmospheric
1017 Chemistry and Physics*, 19, 8897-8913, 10.5194/acp-19-8897-2019, 2019.

1018 Li, W., Li, L., Chen, C.-l., Kacarab, M., Peng, W., Price, D., Xu, J., and Cocker, D. R.:
1019 Potential of select intermediate-volatility organic compounds and consumer products
1020 for secondary organic aerosol and ozone formation under relevant urban conditions,
1021 *Atmospheric Environment*, 178, 109-117, 10.1016/j.atmosenv.2017.12.019, 2018.
1022 Li, X.-B., Yuan, B., Wang, S., Wang, C., Lan, J., Liu, Z., Song, Y., He, X., Huangfu, Y.,
1023 Pei, C., Cheng, P., Yang, S., Qi, J., Wu, C., Huang, S., You, Y., Chang, M., Zheng, H.,
1024 Yang, W., Wang, X., and Shao, M.: Variations and sources of volatile organic
1025 compounds (VOCs) in urban region: insights from measurements on a tall tower,
1026 *Atmospheric Chemistry and Physics*, 22, 10567-10587, 10.5194/acp-22-10567-2022,
1027 2022.
1028 Li, X.-B., Zhang, C., Liu, A., Yuan, B., Yang, H., Liu, C., Wang, S., Huangfu, Y., Qi, J.,
1029 Liu, Z., He, X., Song, X., Chen, Y., Peng, Y., Zhang, X., Zheng, E., Yang, L., Yang, Q.,
1030 Qin, G., Zhou, J., and Shao, M.: Assessment of long tubing in measuring atmospheric
1031 trace gases: applications on tall towers, *Environmental Science: Atmospheres*,
1032 10.1039/d2ea00110a, 2023.
1033 Li, Y., Pöschl, U., and Shiraiwa, M.: Molecular corridors and parameterizations of
1034 volatility in the chemical evolution of organic aerosols, *Atmospheric Chemistry and*
1035 *Physics*, 16, 3327-3344, 10.5194/acp-16-3327-2016, 2016.
1036 Liang, Z., Chen, L., Alam, M. S., Zeraati Rezaei, S., Stark, C., Xu, H., and Harrison, R.
1037 M.: Comprehensive chemical characterization of lubricating oils used in modern
1038 vehicular engines utilizing GC × GC-TOFMS, *Fuel*, 220, 792-799,
1039 10.1016/j.fuel.2017.11.142, 2018.
1040 Liu, Y., Li, Y., Yuan, Z., Wang, H., Sha, Q., Lou, S., Liu, Y., Hao, Y., Duan, L., Ye, P.,
1041 Zheng, J., Yuan, B., and Shao, M.: Identification of two main origins of intermediate-
1042 volatility organic compound emissions from vehicles in China through two-phase
1043 simultaneous characterization, *Environ Pollut*, 281, 117020,
1044 10.1016/j.envpol.2021.117020, 2021.
1045 Malherbe, L., and Mandin, C.: VOC emissions during outdoor ship painting and health-
1046 risk assessment, *Atmospheric Environment*, 41, 6322-6330,
1047 10.1016/j.atmosenv.2007.02.018, 2007.
1048 McDonald, B. C., de Gouw, J. A., Gilman, J. B., Jathar, S. H., Akherati, A., Cappa, C.
1049 D., Jimenez, J. L., Lee-Taylor, J., Hayes, P. L., McKeen, S. A., Cui, Y. Y., Kim, S.-W.,
1050 Gentner, D. R., Isaacman-VanWertz, G., Goldstein, A. H., Harley, R. A., Frost, G. J.,
1051 Roberts, J. M., Ryerson, T. B., and Trainer, M.: Volatile chemical products emerging as
1052 largest petrochemical source of urban organic emissions, *Science*, 359, 760,
1053 10.1126/science.aaq0524, 2018.
1054 Mo, Z., Shao, M., and Lu, S.: Compilation of a source profile database for hydrocarbon
1055 and OVOC emissions in China, *Atmospheric Environment*, 143, 209-217,
1056 10.1016/j.atmosenv.2016.08.025, 2016.
1057 Mo, Z., Cui, R., Yuan, B., Cai, H., McDonald, B. C., Li, M., Zheng, J., and Shao, M.:
1058 A mass-balance-based emission inventory of non-methane volatile organic compounds
1059 (NMVOCs) for solvent use in China, *Atmospheric Chemistry and Physics*, 21, 13655-
1060 13666, 10.5194/acp-21-13655-2021, 2021.

1061 Na, K., and Pyo Kim, Y.: Chemical mass balance receptor model applied to ambient
1062 C₂–C₉ VOC concentration in Seoul, Korea: Effect of chemical reaction losses,
1063 *Atmospheric Environment*, 41, 6715-6728,
1064 <https://doi.org/10.1016/j.atmosenv.2007.04.054>, 2007.

1065 Ou, J., Zheng, J., Li, R., Huang, X., Zhong, Z., Zhong, L., and Lin, H.: Speciated OVOC
1066 and VOC emission inventories and their implications for reactivity-based ozone control
1067 strategy in the Pearl River Delta region, China, *Sci Total Environ*, 530-531, 393-402,
1068 10.1016/j.scitotenv.2015.05.062, 2015.

1069 Qin, M., Murphy, B. N., Isaacs, K. K., McDonald, B. C., Lu, Q., McKeen, S. A., Koval,
1070 L., Robinson, A. L., Efstathiou, C., Allen, C., and Pye, H. O. T.: Criteria pollutant
1071 impacts of volatile chemical products informed by near-field modelling, *Nature*
1072 *Sustainability*, 4, 129-137, 10.1038/s41893-020-00614-1, 2021.

1073 Rogers, T. M., Grimsrud, E. P., Herndon, S. C., Jayne, J. T., Kolb, C. E., Allwine, E.,
1074 Westberg, H., Lamb, B. K., Zavala, M., Molina, L. T., Molina, M. J., and Knighton, W.
1075 B.: On-road measurements of volatile organic compounds in the Mexico City
1076 metropolitan area using proton transfer reaction mass spectrometry, *International*
1077 *Journal of Mass Spectrometry*, 252, 26-37, 10.1016/j.ijms.2006.01.027, 2006.

1078 Sasidharan, S., He, Y., Akherati, A., Li, Q., Li, W., Cocker, D., McDonald, B. C.,
1079 Coggon, M. M., Seltzer, K. M., Pye, H. O. T., Pierce, J. R., and Jathar, S. H.: Secondary
1080 Organic Aerosol Formation from Volatile Chemical Product Emissions: Model
1081 Parameters and Contributions to Anthropogenic Aerosol, *Environmental Science &*
1082 *Technology*, 57, 11891-11902, 10.1021/acs.est.3c00683, 2023.

1083 Seco, R., Peñuelas, J., Filella, I., Llusà, J., Molowny-Horas, R., Schallhart, S., Metzger,
1084 A., Müller, M., and Hansel, A.: Contrasting winter and summer VOC mixing ratios at
1085 a forest site in the Western Mediterranean Basin: the effect of local biogenic emissions,
1086 *Atmospheric Chemistry and Physics*, 11, 13161-13179, 10.5194/acp-11-13161-2011,
1087 2011.

1088 Sekimoto, K., Li, S.-M., Yuan, B., Koss, A., Coggon, M., Warneke, C., and de Gouw,
1089 J.: Calculation of the sensitivity of proton-transfer-reaction mass spectrometry (PTR-
1090 MS) for organic trace gases using molecular properties, *International Journal of Mass*
1091 *Spectrometry*, 421, 71-94, 10.1016/j.ijms.2017.04.006, 2017.

1092 Seltzer, K. M., Pennington, E., Rao, V., Murphy, B. N., Strum, M., Isaacs, K. K., and
1093 Pye, H. O. T.: Reactive organic carbon emissions from volatile chemical products,
1094 *Atmos Chem Phys*, 21, 5079-5100, 10.5194/acp-21-5079-2021, 2021.

1095 Seltzer, K. M., Murphy, B. N., Pennington, E. A., Allen, C., Talgo, K., and Pye, H. O.
1096 T.: Volatile Chemical Product Enhancements to Criteria Pollutants in the United States,
1097 *Environ Sci Technol*, 56, 6905-6913, 10.1021/acs.est.1c04298, 2022.

1098 Sha, Q., Zhu, M., Huang, H., Wang, Y., Huang, Z., Zhang, X., Tang, M., Lu, M., Chen,
1099 C., Shi, B., Chen, Z., Wu, L., Zhong, Z., Li, C., Xu, Y., Yu, F., Jia, G., Liao, S., Cui, X.,
1100 Liu, J., and Zheng, J.: A newly integrated dataset of volatile organic compounds (VOCs)
1101 source profiles and implications for the future development of VOCs profiles in China,
1102 *Sci Total Environ*, 793, 148348, 10.1016/j.scitotenv.2021.148348, 2021.

1103 Shi, Y., Xi, Z., Lv, D., Simayi, M., Liang, Y., Ren, J., and Xie, S.: Sector-based volatile
1104 organic compound emission characteristics and reduction perspectives for coating

1105 materials manufacturing in China, *Journal of Cleaner Production*, 394,
1106 10.1016/j.jclepro.2023.136407, 2023.

1107 Song, X., Yuan, B., Wang, S., He, X., Li, X., Peng, Y., Chen, Y., Qi, J., Cai, J., Huang,
1108 s., Hu, D., Wei, W., Liu, K., and Shao, M.: Compositional Characteristics of Volatile
1109 Organic Compounds in Typical Industrial Areas of the Pearl River Delta: Importance
1110 of Oxygenated Volatile Organic Compounds (in Chinese), *Environmental Science*,
1111 10.13227/j.hjlx.202204104, 2023.

1112 Stark, H., Yatavelli, R. L. N., Thompson, S. L., Kimmel, J. R., Cubison, M. J., Chhabra,
1113 P. S., Canagaratna, M. R., Jayne, J. T., Worsnop, D. R., and Jimenez, J. L.: Methods to
1114 extract molecular and bulk chemical information from series of complex mass spectra
1115 with limited mass resolution, *International Journal of Mass Spectrometry*, 389, 26-38,
1116 10.1016/j.ijms.2015.08.011, 2015.

1117 Stockwell, C. E., Coggon, M. M., Gkatzelis, G. I., Ortega, J., McDonald, B. C., Peischl,
1118 J., Aikin, K., Gilman, J. B., Trainer, M., and Warneke, C.: Volatile organic compound
1119 emissions from solvent- and water-borne coatings – compositional differences and
1120 tracer compound identifications, *Atmospheric Chemistry and Physics*, 21, 6005-6022,
1121 10.5194/acp-21-6005-2021, 2021.

1122 Sulzer, P., Hartungen, E., Hanel, G., Feil, S., Winkler, K., Mutschlechner, P., Haidacher,
1123 S., Schotchkowsky, R., Gunsch, D., Seehauser, H., Striednig, M., Jürschik, S., Breiev, K.,
1124 Lanza, M., Herbig, J., Märk, L., Märk, T. D., and Jordan, A.: A Proton Transfer
1125 Reaction-Quadrupole interface Time-Of-Flight Mass Spectrometer (PTR-QiTOF):
1126 High speed due to extreme sensitivity, *International Journal of Mass Spectrometry*, 368,
1127 1-5, 10.1016/j.ijms.2014.05.004, 2014.

1128 Sun, W., Shao, M., Granier, C., Liu, Y., Ye, C. S., and Zheng, J. Y.: Long-Term Trends
1129 of Anthropogenic SO₂, NO_x, CO, and NMVOCs Emissions in China, *Earth's Future*, 6,
1130 1112-1133, 10.1029/2018ef000822, 2018.

1131 Tan, Y., Han, S., Chen, Y., Zhang, Z., Li, H., Li, W., Yuan, Q., Li, X., Wang, T., and Lee,
1132 S.-c.: Characteristics and source apportionment of volatile organic compounds (VOCs)
1133 at a coastal site in Hong Kong, *Science of The Total Environment*, 777,
1134 10.1016/j.scitotenv.2021.146241, 2021.

1135 Ulbrich, I. M., Canagaratna, M. R., Zhang, Q., Worsnop, D. R., and Jimenez, J. L.:
1136 Interpretation of organic components from Positive Matrix Factorization of aerosol
1137 mass spectrometric data, *Atmos. Chem. Phys.*, 9, 2891-2918, 10.5194/acp-9-2891-2009,
1138 2009.

1139 Wang, C., Yuan, B., Wu, C., Wang, S., Qi, J., Wang, B., Wang, Z., Hu, W., Chen, W.,
1140 Ye, C., Wang, W., Sun, Y., Wang, C., Huang, S., Song, W., Wang, X., Yang, S., Zhang,
1141 S., Xu, W., Ma, N., Zhang, Z., Jiang, B., Su, H., Cheng, Y., Wang, X., and Shao, M.:
1142 Measurements of higher alkanes using NO⁺ chemical ionization in PTR-ToF-MS:
1143 important contributions of higher alkanes to secondary organic aerosols in China,
1144 *Atmospheric Chemistry and Physics*, 20, 14123-14138, 10.5194/acp-20-14123-2020,
1145 2020.

1146 Wang, H., Qiao, Y., Chen, C., Lu, J., Dai, H., Qiao, L., Lou, S., Huang, C., Li, L., Jing,
1147 S., and Wu, J.: Source Profiles and Chemical Reactivity of Volatile Organic Compounds

1148 from Solvent Use in Shanghai, China, *Aerosol and Air Quality Research*, 14, 301-310,
1149 10.4209/aaqr.2013.03.0064, 2014.

1150 Wang, H., Sun, S., Nie, L., Zhang, Z., Li, W., and Hao, Z.: A review of whole-process
1151 control of industrial volatile organic compounds in China, *Journal of Environmental*
1152 *Sciences*, 123, 127-139, 10.1016/j.jes.2022.02.037, 2023.

1153 Wang, R., Zhang, C., Ding, H., LV, S., Ding, Y., Wang, H., and Wang, B.: Emission
1154 characteristics of volatile organic compounds (VOCs) from the production processes of
1155 plastic parts in electronic manufacturing industry (in Chinese), *Acta Scientiae*
1156 *Circumstantiae*, 39, 4-12, 10.13671/j.hjkxxb.2018.0243, 2019.

1157 Wang, S., Yuan, B., Wu, C., Wang, C., Li, T., He, X., Huangfu, Y., Qi, J., Li, X. B., Sha,
1158 Q., Zhu, M., Lou, S., Wang, H., Karl, T., Graus, M., Yuan, Z., and Shao, M.: Oxygenated
1159 volatile organic compounds (VOCs) as significant but varied contributors to VOC
1160 emissions from vehicles, *Atmos. Chem. Phys.*, 22, 9703-9720, 10.5194/acp-22-9703-
1161 2022, 2022.

1162 Wei, W., Wang, S., Hao, J., and Cheng, S.: Projection of anthropogenic volatile organic
1163 compounds (VOCs) emissions in China for the period 2010–2020, *Atmospheric*
1164 *Environment*, 45, 6863-6871, <https://doi.org/10.1016/j.atmosenv.2011.01.013>, 2011.

1165 Wu, C., Wang, C., Wang, S., Wang, W., Yuan, B., Qi, J., Wang, B., Wang, H., Wang, C.,
1166 Song, W., Wang, X., Hu, W., Lou, S., Ye, C., Peng, Y., Wang, Z., Huangfu, Y., Xie, Y.,
1167 Zhu, M., Zheng, J., Wang, X., Jiang, B., Zhang, Z., and Shao, M.: Measurement report:
1168 Important contributions of oxygenated compounds to emissions and chemistry of
1169 volatile organic compounds in urban air, *Atmospheric Chemistry and Physics*, 20,
1170 14769-14785, 10.5194/acp-20-14769-2020, 2020a.

1171 Wu, J., Gao, S., Chen, X., Yang, Y., Fu, Q.-y., Che, X., and Jiao, Z.: Source Profiles and
1172 Impact of Volatile Organic Compounds in the Coating Manufacturing Industry (in
1173 Chinese), *Environmental Science*, 41, 1582-1588, 10.13227/j.hjkx.201908203, 2020b.

1174 Yang, G., Huo, J., Wang, L., Wang, Y., Wu, S., Yao, L., Fu, Q., and Wang, L.: Total OH
1175 Reactivity Measurements in a Suburban Site of Shanghai, *Journal of Geophysical*
1176 *Research: Atmospheres*, 127, 10.1029/2021jd035981, 2022.

1177 Yang, Y., Shao, M., Wang, X., Nölscher, A. C., Kessel, S., Guenther, A., and Williams,
1178 J.: Towards a quantitative understanding of total OH reactivity: A review, *Atmospheric*
1179 *Environment*, 134, 147-161, <https://doi.org/10.1016/j.atmosenv.2016.03.010>, 2016.

1180 Yuan, B., Shao, M., Lu, S., and Wang, B.: Source profiles of volatile organic compounds
1181 associated with solvent use in Beijing, China, *Atmospheric Environment*, 44, 1919-
1182 1926, 10.1016/j.atmosenv.2010.02.014, 2010.

1183 Yuan, B., Shao, M., Gouw, J. D., Parrish, D. D., Lu, S., Wang, M., Zeng, L., Zhang, Q.,
1184 Song, Y., and Zhang, J.: Volatile organic compounds (VOCs) in urban air: How
1185 chemistry affects the interpretation of positive matrix factorization (PMF) analysis,
1186 *Journal of Geophysical Research Atmospheres*, 117, 24302, 2012.

1187 Yuan, B., Koss, A. R., Warneke, C., Coggon, M., Sekimoto, K., and de Gouw, J. A.:
1188 Proton-Transfer-Reaction Mass Spectrometry: Applications in Atmospheric Sciences,
1189 *Chemical Reviews*, 117, 13187-13229, 10.1021/acs.chemrev.7b00325, 2017.

1190 Zhao, J., Yao, X., Sun, M., Xu, Y., Wang, S., Cao, D., and Liu, J.: Emission
1191 characteristics of volatile organic compounds from typical solvent use industries in

1192 Tianjin (in Chinese), *Environmental Pollution & Control*, 43, 539-545,
1193 10.15985/j.cnki.1001-3865.2021.05.002, 2021.

1194 Zhao, R., Huang, L., Zhang, J., and Ouyang, F.: Emissions characteristics of volatile
1195 organic compounds (VOCs) from typical industries of solvent use in Chengdu City (in
1196 Chinese), *Acta Scientiae Circumstantiae*, 38, 1147-1154, 10.13671 /j.hjkxxb.2017.0362,
1197 2018a.

1198 Zhao, Y., Hennigan, C. J., May, A. A., Tkacik, D. S., de Gouw, J. A., Gilman, J. B.,
1199 Kuster, W. C., Borbon, A., and Robinson, A. L.: Intermediate-volatility organic
1200 compounds: a large source of secondary organic aerosol, *Environ Sci Technol*, 48,
1201 13743-13750, 10.1021/es5035188, 2014.

1202 Zhao, Y., Nguyen, N. T., Presto, A. A., Hennigan, C. J., May, A. A., and Robinson, A.
1203 L.: Intermediate Volatility Organic Compound Emissions from On-Road Gasoline
1204 Vehicles and Small Off-Road Gasoline Engines, *Environmental Science & Technology*,
1205 50, 4554-4563, 10.1021/acs.est.5b06247, 2016.

1206 Zhao, Y., Lambe, A. T., Saleh, R., Saliba, G., and Robinson, A. L.: Secondary Organic
1207 Aerosol Production from Gasoline Vehicle Exhaust: Effects of Engine Technology,
1208 Cold Start, and Emission Certification Standard, *Environ Sci Technol*, 52, 1253-1261,
1209 10.1021/acs.est.7b05045, 2018b.

1210 Zheng, J., Yu, Y., Mo, Z., Zhang, Z., Wang, X., Yin, S., Peng, K., Yang, Y., Feng, X.,
1211 and Cai, H.: Industrial sector-based volatile organic compound (VOC) source profiles
1212 measured in manufacturing facilities in the Pearl River Delta, China, *Sci Total Environ*,
1213 456-457, 127-136, 10.1016/j.scitotenv.2013.03.055, 2013.

1214 Zhong, Z., Sha, Q., Zheng, J., Yuan, Z., Gao, Z., Ou, J., Zheng, Z., Li, C., and Huang,
1215 Z.: Sector-based VOCs emission factors and source profiles for the surface coating
1216 industry in the Pearl River Delta region of China, *Sci Total Environ*, 583, 19-28,
1217 10.1016/j.scitotenv.2016.12.172, 2017.

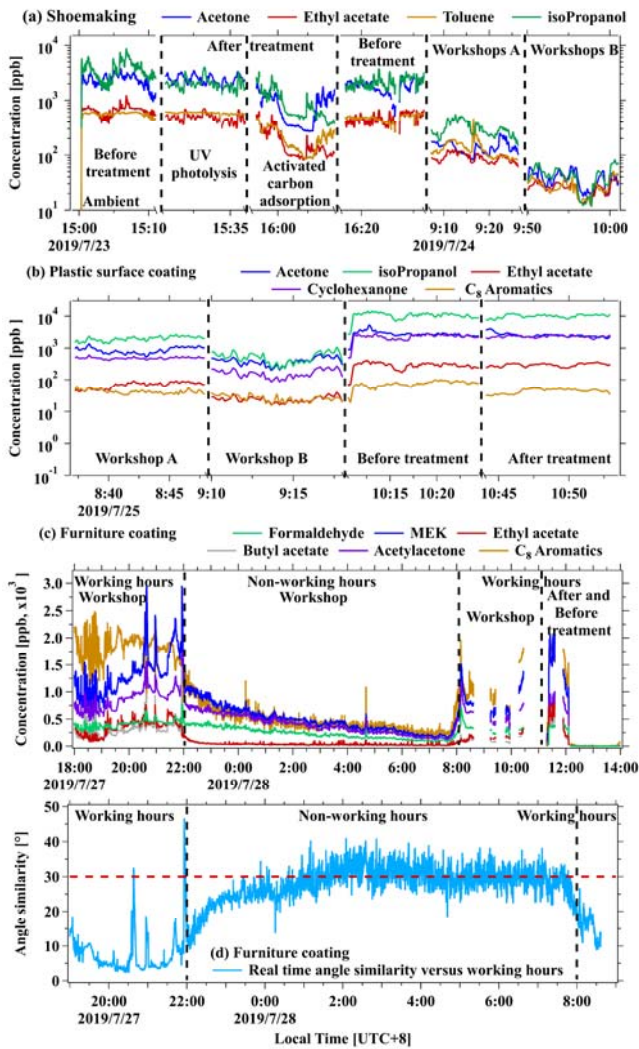
1218 Zhong, Z., Zheng, J., Zhu, M., Huang, Z., Zhang, Z., Jia, G., Wang, X., Bian, Y., Wang,
1219 Y., and Li, N.: Recent developments of anthropogenic air pollutant emission inventories
1220 in Guangdong province, China, *Sci Total Environ*, 627, 1080-1092,
1221 10.1016/j.scitotenv.2018.01.268, 2018.

1222 Zhou, Z., Deng, Y., Zhou, X., Wu, K., TAN, Q., Yin, D., Song, D., Chen, Q., and Zeng,
1223 W.: Source Profiles of Industrial Emission-Based VOCs in Chengdu (in Chinese),
1224 *Environmental Science*, 41, 3042-3055, 10.13227/j.hjkx.201912203, 2020a.

1225 Zhou, Z., Tan, Q., Deng, Y., Song, D., Wu, K., Zhou, X., Huang, F., Zeng, W., and Lu,
1226 C.: Compilation of emission inventory and source profile database for volatile organic
1227 compounds: A case study for Sichuan, China, *Atmospheric Pollution Research*, 11, 105-
1228 116, <https://doi.org/10.1016/j.apr.2019.09.020>, 2020b.

1229 Zhu, W., Guo, S., Zhang, Z., Wang, H., Yu, Y., Chen, Z., Shen, R., Tan, R., Song, K.,
1230 Liu, K., Tang, R., Liu, Y., Lou, S., Li, Y., Zhang, W., Zhang, Z., Shuai, S., Xu, H., Li,
1231 S., Chen, Y., Hu, M., Canonaco, F., and Prévôt, A. S. H.: Mass spectral characterization
1232 of secondary organic aerosol from urban cooking and vehicular sources, *Atmospheric
1233 Chemistry and Physics*, 21, 15065-15079, 10.5194/acp-21-15065-2021, 2021.

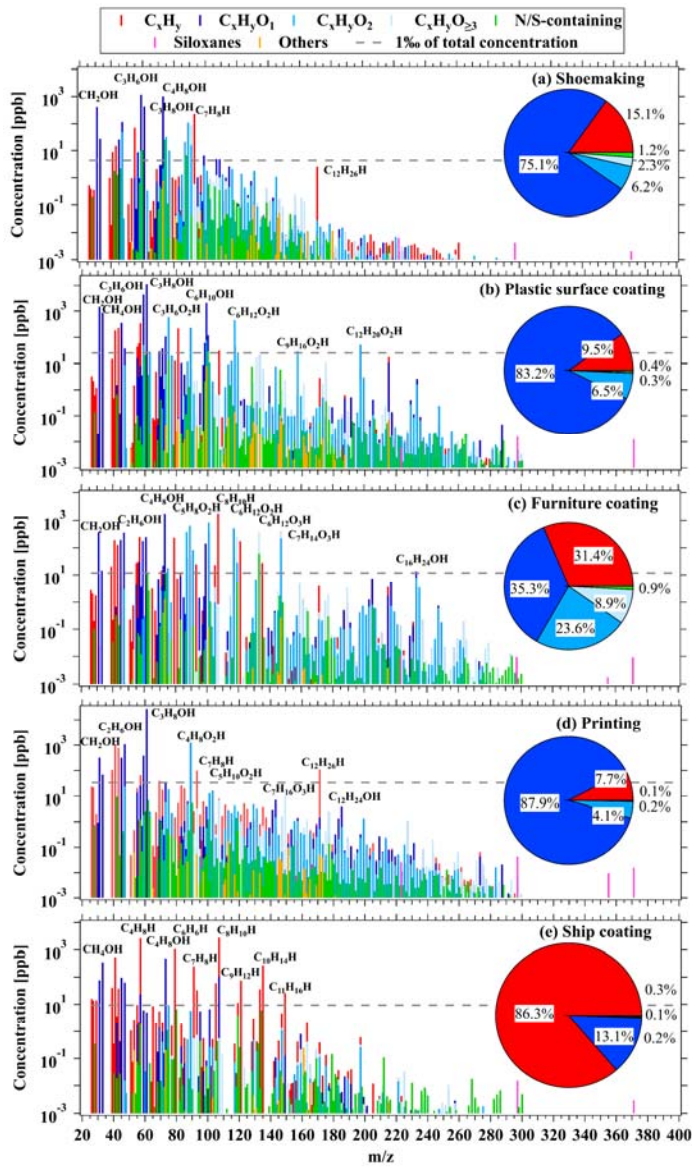
1234



删除了: and

1235
 1236 **Figure 1.** Real-time concentrations of representative ROG from workshops, before
 1237 and after the ROG treatment devices in (a) shoe making industry, (b) plastic surface
 1238 coating industry, and (c) during working hours or non-working hours in the furniture
 1239 coating industry. (d) The θ angles of mass spectra among real-time concentrations
 1240 versus average concentration during working time (19:00-22:00) in the furniture
 1241 coating industry.

1242



1244

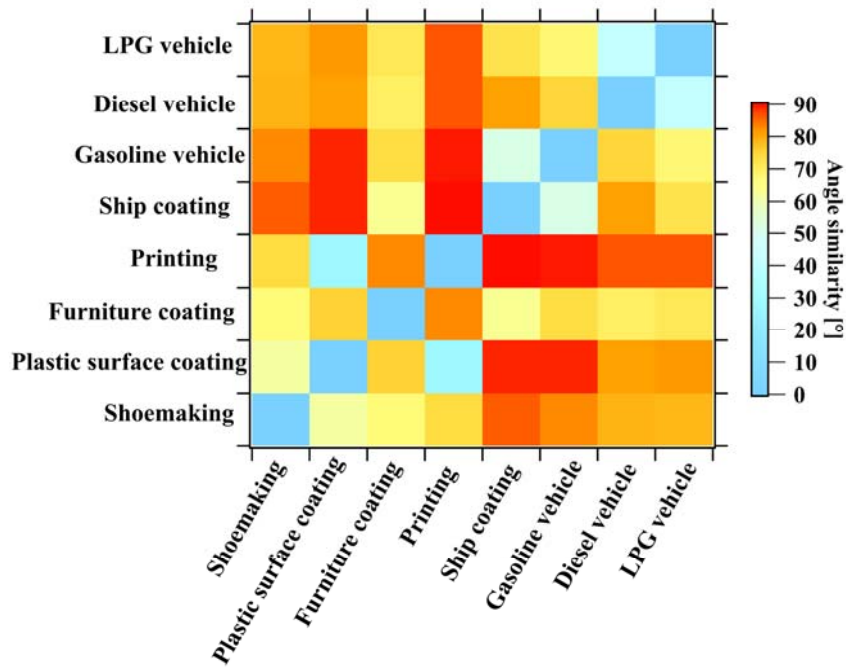
1245 **Figure 2.** Average concentrations and fractions of ROGs measured by PTR-ToF-MS

1246 from stack emissions in (a) shoemaking, (b) plastic surface coating, (c) furniture coating,

1247 (d) printing, and (e) ship coating industries.

1248

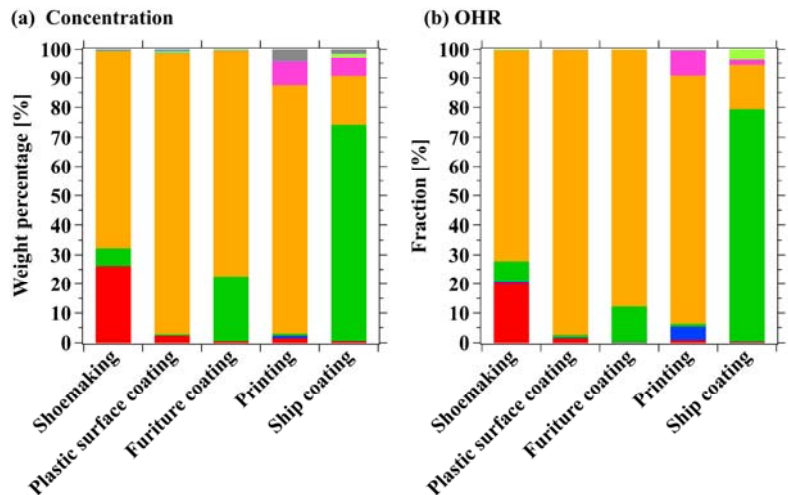
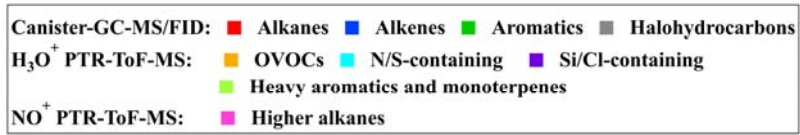
删除了: of



1250
 1251 **Figure 3.** The θ angles among the mass spectra of industrial VCP sources in this study
 1252 and vehicular emissions from previous study (Wang et al., 2022).

删除了: (°)

1253



1255

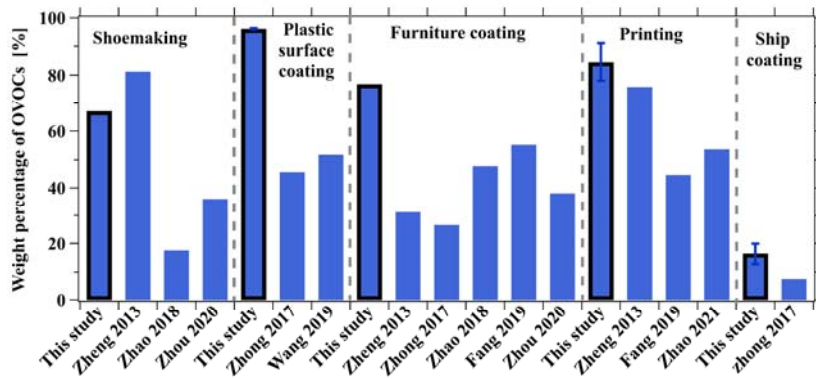
1256 **Figure 4.** Fractions of (a) concentrations and (b) OHR for ROG components to total

1257 ROGs from stack emissions in shoemaking, plastic surface coating, furniture coating,

1258 printing, and ship coating industries.

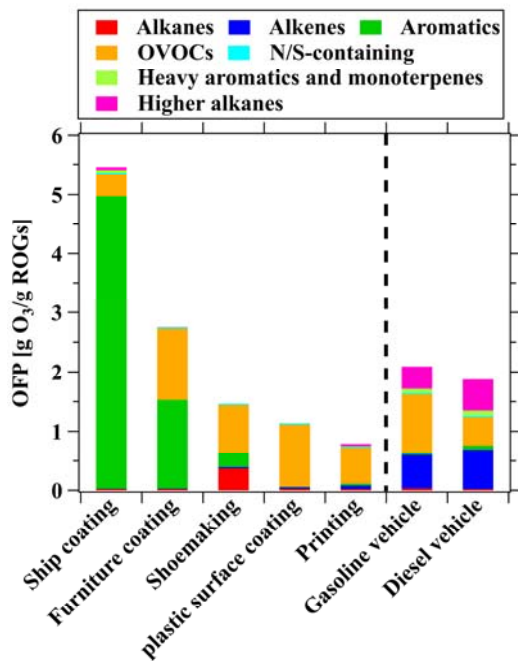
1259

删除了: from

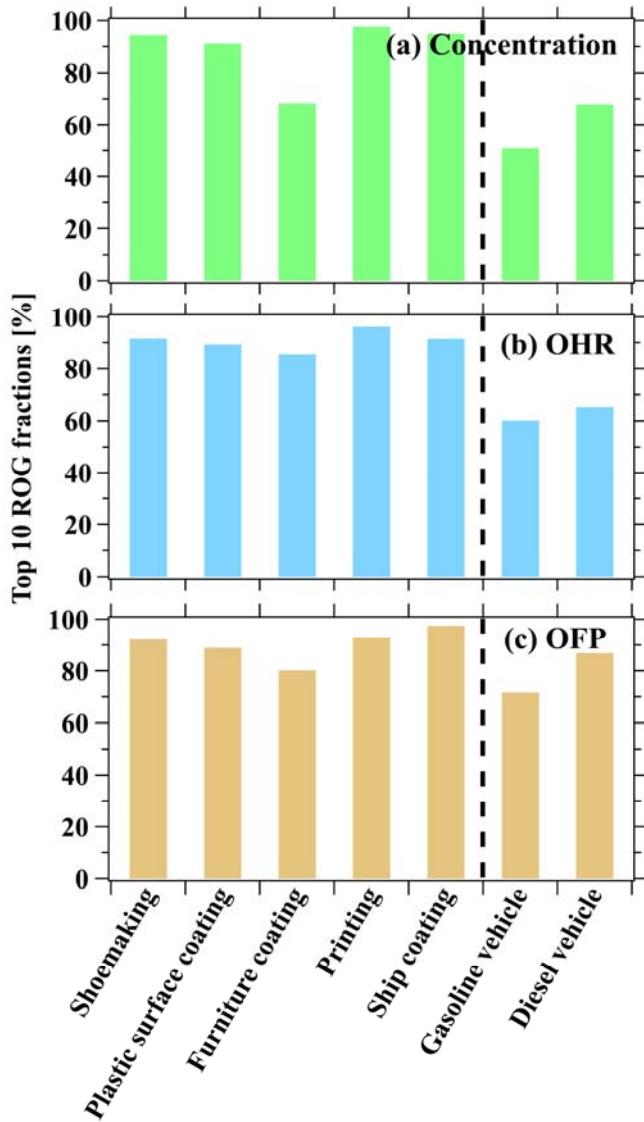


1261

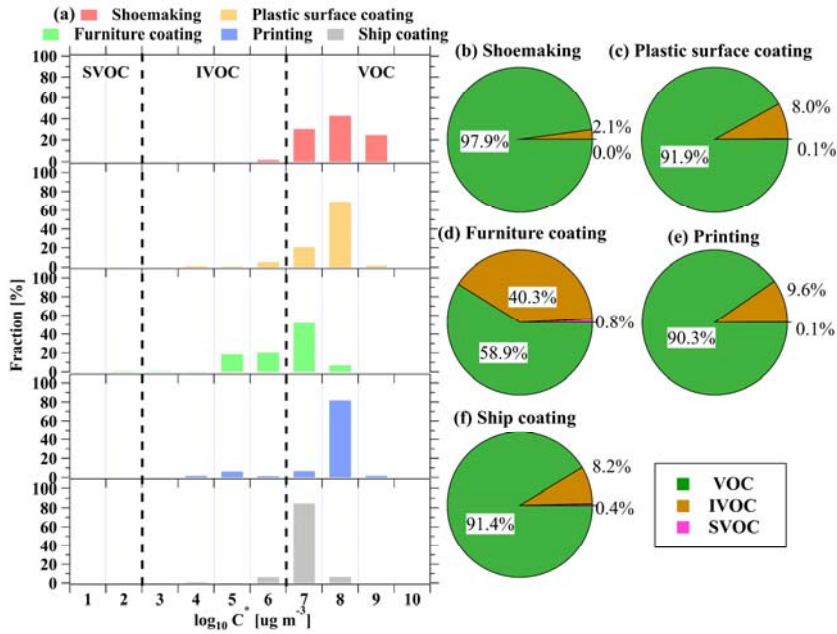
1262 **Figure 5.** Comparison of OVOC fractions determined from stack emission of industrial
 1263 VCP sources in this study and those in previous studies. Error bars represent the
 1264 standard deviations of the weight percentage of OVOCs.
 1265



1266
 1267 **Figure 6.** Comparison of OFP among various industrial VCP sources in this study and
 1268 vehicular emissions from previous study (Wang et al., 2022).
 1269



1270
 1271 **Figure 7.** Accumulated fractions of the top ten species in total (a) ROG emissions, (b)
 1272 OHR, and (c) OFP from industrial VCP sources in this study and vehicular emissions
 1273 from previous study (Wang et al., 2022).
 1274

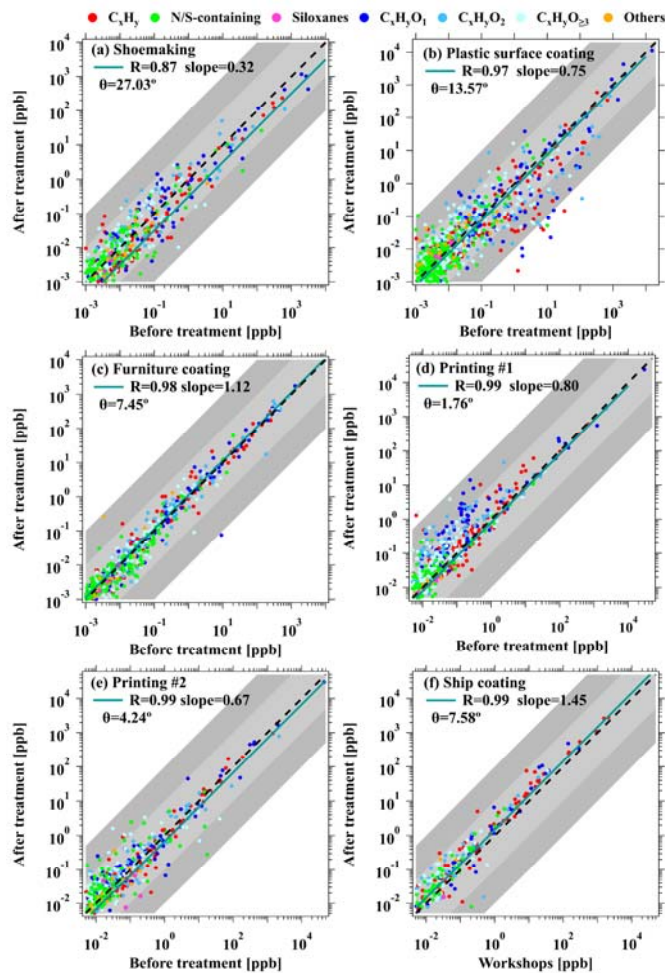


1275
 1276 **Figure 8.** (a) Volatility-binned fractions from stack emissions of various industrial VCP
 1277 sources, and volatility-binned fractions ~~from~~ different ROG categories ~~in~~ (b)
 1278 shoemaking, (c) plastic surface coating, (d) furniture coating, (e) printing, and (f) ship
 1279 coating industries.

删除了: in

删除了: from stack emissions of

1280
 1281

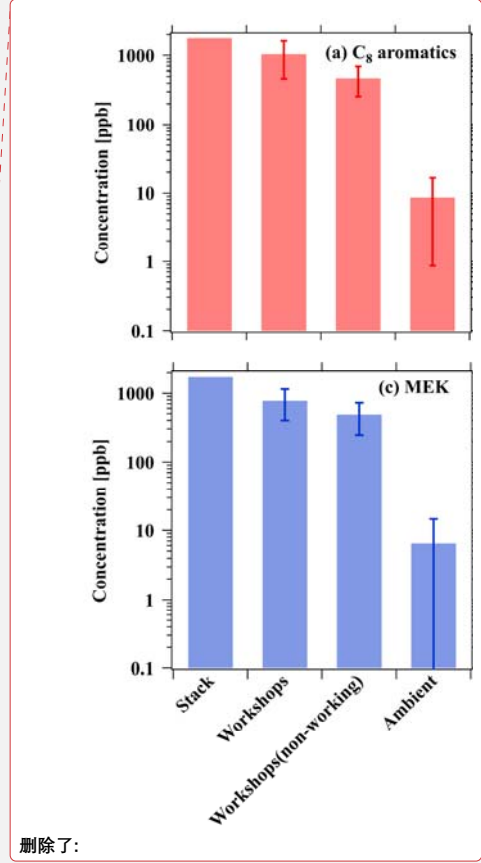
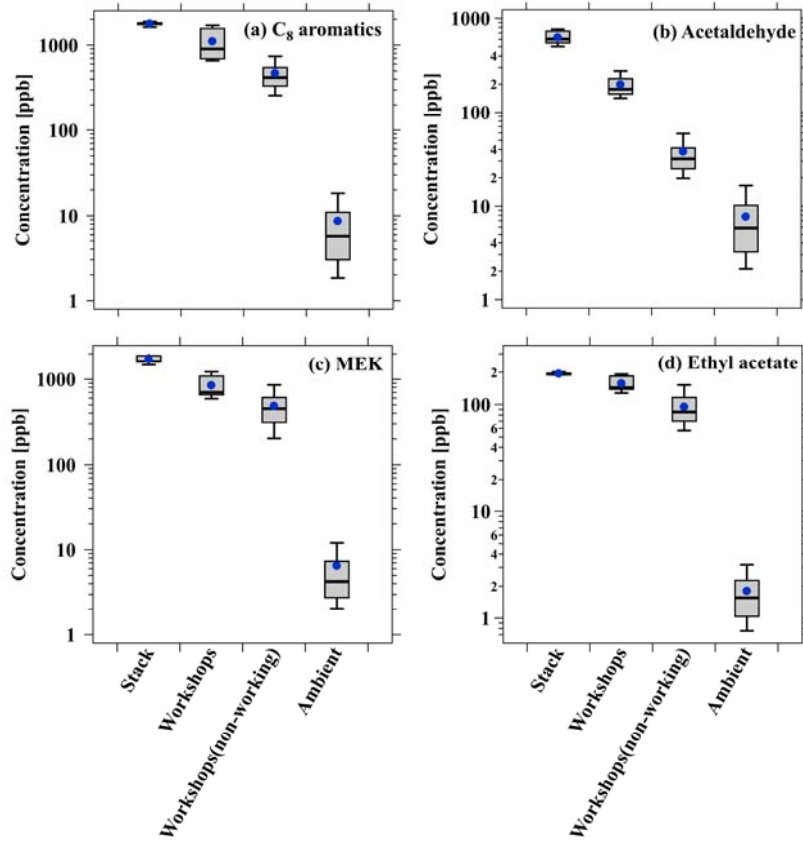


1284
 1285 **Figure 9.** Scatterplots of ROG concentrations between before and after treatment with
 1286 activated carbon adsorption + UV photolysis in (a) shoemaking, (b) plastics surface
 1287 coating, (c) furniture coating, and (d) printing industries. Scatterplots of ROG
 1288 concentrations between before and after treatment with catalytic combustion in (e) the
 1289 printing industry, and ROG concentrations between workshops and after treatment with
 1290 catalytic combustion in (f) the ship coating industry. The green lines are the fitted
 1291 results for all data points. The black dashed lines represent 1:1 ratio, and the shaded
 1292 areas represent ratios of a factor of 10 and 100.

1293

删除了: for

删除了: for

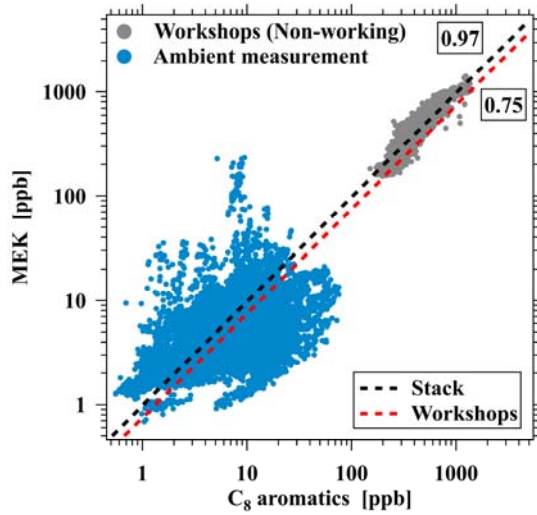


删除了:

- 删除了: Average
- 删除了: concentrations
- 删除了: of
- 删除了: emission
- 删除了: from
- 删除了: Error bars represent the standard deviations of the concentration.

1296
 1297 **Figure 10.** Boxplots of (a) C₈ aromatics, (b) acetaldehyde, (c) MEK, and (d) ethyl
 1298 acetate concentrations, across the stack, workshops during working and non-working
 1299 hours in the furniture coating industry, and ambient measurement near the industry,
 1300 respectively.

1301



1310
 1311
 1312
 1313
 1314
 1315

Figure 11. Scatterplot of MEK versus C₈ aromatic concentrations from workshops during non-working hours in the furniture coating industry and ambient measurement near the industry. The black and red dashed line represent ratios of ROG pairs for stack and workshops emission in furniture coating industry.

删除了: s
 删除了: at